NASA TECHNICAL NOTE

NASA TN D-2270

C. 1



NASA TN D-2270

# FLIGHT TEST PERFORMANCE AND DESCRIPTION OF A ROCKET VEHICLE FOR PRODUCING LOW-SPEED ARTIFICIAL METEORS

*by Clarence A. Brown, Jr., and Jean C. Keating*

*Langley Research Center*

*Langley Station, Hampton, Va.*

NATIONAL AERONAUTICS AND SPACE ADMINISTRATION • WASHINGTON, D. C. • APRIL 1964

# FLIGHT TEST PERFORMANCE AND DESCRIPTION OF A ROCKET VEHICLE FOR PRODUCING LOW-SPEED ARTIFICIAL METEORS

By Clarence A. Brown, Jr., and Jean C. Keating

Langley Research Center
Langley Station, Hampton, Va.

NATIONAL AERONAUTICS AND SPACE ADMINISTRATION

For sale by the Office of Technical Services, Department of Commerce,
Washington, D.C. 20230 -- Price $1.25

# FLIGHT TEST PERFORMANCE AND DESCRIPTION OF A ROCKET VEHICLE FOR PRODUCING LOW-SPEED ARTIFICIAL METEORS

By Clarence A. Brown, Jr., and Jean C. Keating
Langley Research Center

## SUMMARY

The six-stage Trailblazer I vehicle with a seventh-stage shaped-charge accelerator developed by the Air Force Cambridge Research Laboratories was successful in producing an artificial low-speed iron meteoroid that reached a velocity at reentry of 32,100 feet per second. The flight test was conducted at the NASA Wallops Station, Wallops Island, Virginia, and indicated that the performance of the vehicle was very close to the values indicated by preflight calculations. Optical data were obtained at three camera sites and yielded data necessary to compute for the first time the luminous efficiency of an artificial iron meteoroid reentering the atmosphere.

## INTRODUCTION

Artificial iron meteoroids are of current interest to meteor physicists and astronomers since many photographic plates of meteors of unknown mass and composition have been obtained. Some knowledge of the mass, composition, and shape has been obtained from meteorites - stony or metallic bodies that have reached the surface of the earth without being completely vaporized - but assumptions must be made as to the size, shape, and composition of the meteors during the reentry. In order to make better use of the photographic plates of meteors, it was first necessary to obtain within narrower limits than previously available, the efficiency with which the kinetic energy of a meteoroid is transformed to luminous energy in the photographic region; this is called the luminous efficiency of a meteoroid. The photographic intensity of the luminous energy and velocity of the meteoroid can be obtained by observation, but in order to compute the mass of a natural meteor, a determination of the luminosity coefficient of the meteor must be obtained. Many different elements have been detected in natural meteors from spectrographic plates and one element of interest is iron. As pointed out in reference 1, observations of natural meteors have not yet yielded reliable data on the luminous efficiency, meteor masses, or meteor densities. The present experiment was intended to obtain a reliable value of the luminous efficiency of one meteor element, iron. The vehicle used to reenter such a low-speed meteoroid is described herein.

The unique six-stage, solid-fuel Trailblazer I rocket system was developed to study the physical phenomena which occur during the reentry of high-speed objects into the earth's atmosphere. A detailed review of the vehicle design and a description of the vehicle system are presented in reference 2; the aerodynamic characteristics of the vehicle are given in references 3 and 4. In the first nine flight tests (described in ref. 2) the reentry velocity of the payload varied between 18,000 and 25,000 feet per second.

In order to obtain the increased velocity necessary for meteor simulation, a shaped-charge accelerator, developed by the U.S. Air Force Cambridge Research Laboratories (CRL), was added to the Trailblazer I vehicle as a seventh stage. A description of this seventh-stage, shaped-charge accelerator and the modifications made to the sixth stage are presented herein along with the preliminary trajectory data for this vehicle and the radar data obtained from the flight test.

The Trailblazer reentry research program, of which this vehicle is a part, is a cooperative effort between the NASA and the Massachusetts Institute of Technology - Lincoln Laboratory. Data acquisition and analysis tasks are performed jointly by both organizations. All launchings for the Trailblazer project were conducted at the NASA Wallops Station.

Velocities and altitudes in the text are presented in both English and metric units; a conversion factor of 1 kilometer = 3,280.83 feet was used.

## DESCRIPTION OF ROCKET VEHICLE

A general description of the basic six-stage Trailblazer I configuration is given in reference 2. Further details not included in reference 2 on the fins, the separation mechanics of the stages, and the process used to balance the vehicle dynamically are given in the appendix. The reentry object in the nine flight tests, discussed in reference 2, was the empty sixth-stage 5-inch spherical rocket-motor case. In order to obtain the increased velocity necessary for an artificial meteoroid, a seventh stage was added to the basic Trailblazer configuration hereinafter designated Trailblazer Ig. A sketch and a photograph of the sixth stage and the seventh stage (a shaped-charge accelerator developed by the U.S. Air Force Cambridge Research Laboratories) are shown in figure 1. (See ref. 1.)

The reentry object used to simulate a meteoroid was a 5.8-gram stainless-steel pellet. As can be seen from a sketch in the upper left-hand corner of figure 1(a), the diameter of the front face of the 0.10-inch-thick pellet was 0.83 inch and the diameter of the pellet at the aft end was 0.75 inch. The pellet was mounted in the nose of the seventh stage as shown in figure 2(a).

The seventh-stage accelerator case shown in figure 2(b) and in figure 1 was a 10-inch-long cylinder which was 1.5 inches in diameter and made of 75ST aluminum alloy. The wall thickness of the case was 0.040 inch at the juncture of the 5-inch motor and case, and then tapered to a thickness of 0.010 inch at the pellet end of the case. More than half the length of the shaped-charge accelerator

was used to accommodate a 25-second delay squib. A timer located in the nose of the velocity package simultaneously applied current to the squibs of the fourth, fifth, sixth, and seventh stages. The seventh-stage detonator ignited the 25 grams of tetryl booster. This booster in turn ignited 140 grams of PBX charge which accelerated the pellet to a reentry velocity of approximately 32,000 feet per second.

The seventh-stage shaped-charge accelerator was attached to a boss located on the front of the sixth stage and pinned in place. A sketch of the velocity package, which housed the rearward-firing fourth, fifth, sixth, and seventh stages is shown in figure 3. It was necessary to shorten the fifth-to-sixth stage adaptor used on the vehicle described in reference 2 in order to accommodate the seventh-stage shaped-charge accelerator. A sketch of the complete configuration with dimensions is shown in figure 4, and a photograph of the vehicle in the launch position is shown in figure 5.

Prior to the flight test of Trailblazer Ig, several ground tests were conducted by the U.S. Air Force Cambridge Research Laboratories to determine the effects which the high temperature and blast force produced by the shaped charge would have upon the pellet. These ground tests indicated that the temperature and blast force of the shaped charge resulted in a reduction in both size and mass of the pellet. The average of the results obtained from these tests indicated that the pellet was reduced in mass and diameter to 2.2 grams and 0.575 inch. A photograph of the pellet before and after capture test is presented in figure 6.

## VEHICLE PERFORMANCE

Weights used in computing these trajectories were actual measured weights at vehicle assembly and are presented in table I. The nominal computed trajectory for each stage is shown in figure 7 for the nominal launch angle of 80°. As may be noted in figure 7 the pellet and the sixth-stage 5-inch spherical rocket motor follow essentially the same trajectory and are separated only in time.. The pellet reenters (200,000 feet altitude) approximately 342.5 seconds after launch and the sixth-stage 5-inch spherical rocket motor, 351 seconds after launch. Time notations are included in all trajectories to aid in determination of the position of each stage for any given time after launch. To assure that the vehicle will fly the nominal trajectory (80° launch angle), a computer program was written to adjust the launch elevation and azimuth angles to account for wind variations present at the time of launch. The method is explained in reference 5 for the Trailblazer vehicles.

A time history of the nominal computed vehicle altitude, horizontal range, flight-path angle, and velocity until the time of fourth-stage ignition is shown in figure 8. Pertinent information concerning staging events is also included in a table in this figure. Maximum booster velocity is obtained at third-stage burnout (40.6 seconds) and peak altitude is a direct function of this velocity and flight-path angle. The flight-path angle at third-stage burnout is also the approximate spin-stabilized attitude of the velocity package and

therefore is a major factor in determining the angle of the pellet reentry. The final-stage reentry trajectory is fixed by the combined influence of the vehicle velocity, the flight-path angle, and the velocity-package attitude angle at fourth-stage ignition. Calculated longitudinal acceleration for the ascending portion of the trajectory is presented in figure 9, and curves which show the velocity-time and velocity-altitude relationship for the final four stages during their reentry trajectories are presented in figures 10 and 11, respectively.

## RESULTS OF FLIGHT TEST

The trajectory flown by Trailblazer Ig as obtained by each of the radars used during the flight is shown in figures 12 to 15. Excellent radar data were obtained by the SCR-584, Mod II, FPS-16, and the MIT S-Band radars. Since the Trailblazer configuration is an unguided vehicle, containing no onboard controls for corrections in flight for any deviations from nominal, the vehicle follows an essentially ballistic trajectory. Small changes in the launch azimuth and elevation angles will affect the trajectory in maximum altitude and horizontal range obtained by the vehicle. Since ground-based optical instrumentation was of prime importance for this flight, control of the trajectory was imperative in order to insure optical coverage. Atmospheric winds both at the surface and throughout the atmospheric altitude range have a large effect on trajectory dispersion, a wind compensation method (ref. 5) especially tailored to the vehicle's characteristics was used to determine the launcher settings necessary to compensate for the effects of these winds. The intended trajectory for this vehicle was that of an 80° elevation angle and 150° azimuth angle (measured from true north).

The short range of both the SCR-584 and the Mod II radars limited their coverage of the flight to a short portion of the ascending trajectory. Their purpose was to provide the earliest possible acquisition of the target and yield accurate data on the position of the vehicle during the early part of the flight when the range of the vehicle was below or barely within the minimum range of the long-range tracking radars. From acquisition at 7.5 seconds and 4.0 seconds for the SCR-584 and Mod II, respectively, until the FPS-16 acquired the target at 19 seconds, these short-range radars provided the only radar data available. The FPS-16 retained the target until 200 seconds after launch, at which time the target exceeded the skin tracking range of this radar. The longer range MIT radar, capable of tracking the entire flight, acquired the target at approximately 40 seconds after launch and retained track until after sixth-stage rocket-motor burnout at 320 seconds.

Figures 12, 13, and 14 show the trajectory, flight-path angle, and azimuth angle measured from the launch site by the SCR-584, Mod II, and FPS-16 radars, respectively. Examination of figures 12 to 14 shows that the vehicle flew a trajectory higher in elevation than for the nominal 80° launch-elevation angle, although the launcher setting was corrected for atmospheric winds. The trajectory flown by Trailblazer Ig was approximately equivalent to that which would have resulted from an 81° launch-elevation angle. The azimuth angle differed from the nominal 150° by about 2° after the effects of the atmospheric winds

had been evaluated, and the vehicle had responded to these winds. The flight-path angle shown for all three radars was higher than the nominal for the initial portion of the trajectory, but as may be seen in figure 14(b) it was lower than the nominal after 160 seconds of flight time.

Presented in figure 15 is the trajectory obtained from the MIT S-Band tracking radar. This radar was capable of tracking the vehicle to apogee and indicating the rocket-motor separations on the descending trajectory. The S-Band radar tracked the vehicle to about 324 seconds, or slightly after burnout of the sixth-stage rocket motor. As may be seen in figure 15, the apogee of the trajectory was very close to the nominal, but the horizontal range of the vehicle at apogee was about 100,000 feet closer to the launcher than expected. Comparison of the FPS-16 (fig. 14) and the MIT S-Band (fig. 15) radars shows that the accuracy of the two radars was good.

Vehicle velocity determined from the data of the FPS-16 and the MIT S-Band radars is shown in figures 14(c) and 15(b), respectively. As may be noted from these figures, the velocity obtained agreed closely with the predicted preflight velocity. Velocity data for a portion of the reentry trajectory were obtained from the MIT S-Band radar. The velocity agreed extremely well with the predicted reentry velocity through sixth-stage firing, at which time the radar lost the target. A maximum velocity of 20,500 feet per second was obtained at this time.

Preflight calculations indicated that the spin rate for a $1^{\circ}$ per fin cant ($4^{\circ}$ total angle) of the third-stage fins should be approximately 10 cycles per second. The measured fin cant of the fins was $3^{\circ}51'$ total angle which yielded a maximum spin rate of 9.74 cycles per second as shown in figure 16. This spin rate was determined from the third-stage telemeter and ground-based instrumentation and was adequate for spin stability of the velocity package.

The reentering seventh-stage low-speed iron "meteoroid" was photographed at stations located at Wallops Island, Virginia, Coquina Beach, North Carolina, and Eastville, Virginia. One of the photographs is shown in figure 17 together with a sketch showing the celestial coordinates of the field of view covered by the camera. An analysis of the luminous efficiency of the low-speed artificial iron meteoroid has been made and is presented in reference 6. The iron pellet became visible at an altitude of 226,500 feet (69.04 km). The length of the trail produced by the artificial meteoroid was 21,000 feet (6.40 km). The velocity of the pellet was measured optically and was 32,100 feet per second (9.78 km/sec) (ref. 6). The photograph shown in figure 17 also shows the reentry of the sixth-stage 5-inch spherical rocket motor which, of course, appeared at a later time than did the pellet. This is the first time sufficient data have been obtained to compute the luminous efficiency of an artificial iron meteoroid of a known mass reentering the atmosphere.

Calculations of the heating rates and wall temperatures were made for the seventh-stage pellet by using the method of reference 7 and are presented in figure 18. These calculations were made for both the edge and center of the front face of the pellet.

Reference 6 shows that the pellet became visible at an altitude of 226,500 feet (69.04 km) and remained visible until 205,500 feet (62.64 km). The melting point of stainless steel is 2,750° F and from figure 18 the edge of the pellet reached this temperature at 228,000 feet (69.49 km), very close to the altitude at which the pellet became visible. The center portion of the pellet did not reach this temperature until 213,000 feet (64.92 km) altitude.

## CONCLUDING REMARKS

The six-stage Trailblazer vehicle with a seventh-stage shaped-charge accelerator developed by the U.S. Air Force Cambridge Research Laboratories was successful in producing an artificial low-speed meteoroid that reached a velocity of 32,100 feet per second at reentry. The trajectory and velocity obtained from radar data agreed very well with the preflight predicted values.

Optical data were obtained at three camera sites and yielded data necessary to compute, within narrower limits than previously possible for natural meteors, the luminous efficiency of an artificial iron meteoroid reentering the atmosphere.

Langley Research Center,
National Aeronautics and Space Administration,
Langley Station, Hampton, Va., December 24, 1963.

## APPENDIX

## ADDITIONAL DESCRIPTION OF ROCKET VEHICLE

### First-Stage Booster

The first-stage booster was an Honest John rocket motor with standard cruciform military fins (figs. 19(a) and 20). The fins were of double-wedge section and had the leading edge swept back 42°. The exposed area (that area outside of the rocket motor) for each fin was $7\frac{1}{2}$ square feet per panel. To obtain spin immediately after the vehicle cleared the launcher, four Honest John M-7 spin motors were manifolded together at the forward end of the rocket. These four spin motors produced a spin rate of about 1 cycle per second. In addition to the spin motors, each fin on the Honest John had a cant of approximately one-half degree to maintain this spin rate of 1 to $1\frac{1}{2}$ cycles per second. The first-stage Honest John imparted the spin to the remainder of the vehicle by means of two keys and slots which locked the first and second stages together but did not prevent the stages from drag separating.

### Second-Stage Booster

The second-stage booster was the booster motor of the Nike Ajax missile. The fins, of NASA design, were modified cruciform double-wedge shaped with an exposed area of $2\frac{1}{2}$ square feet per panel (figs. 19(b) and 20). The leading edges of the fins had a sweep angle of 17°. To insure that the leading edge of the fins could withstand the temperature environment of the ascending trajectory, a leading-edge cap of 0.031-inch-thick inconel was added to the fins (fig. 20) for heat protection. The first- and second-stage booster fins were alined because of the position of the stages on the launcher. The second-stage booster fins were not canted to maintain the first-stage spin, but were set as near to zero as manufacturing tolerance would permit. The second and third stages were mechanically held together by a radially slotted thin metal diaphragm which had a threaded flange or rim. The diaphragm was threaded directly into the lip of the third-stage nozzle-exit cone and into the threaded adaptor which was bolted to the forward end of the second stage. At third-stage ignition, the motor exhaust pressure collapsed the diaphragm, disengaged the threads, and permitted the motors to separate. Tip flares were added to the second stage for use as visual acquisition and tracking aids by the radars.

### Third-Stage Booster

The third-stage booster was a TX77 rocket motor with NASA designed fins that were cruciform modified double-wedge shaped and had an exposed area of 2 square feet per panel (fig. 19(c)). The leading edge of the fins was swept back 17° and was obtained by cutting 3.4 inches spanwise from the root chord of

the type of fins used on the second stage (fig. 20). The leading edges were protected from aerodynamic heating by a double cap. This cap was made of 0.031-inch-thick inconel and extended to the flat portion of the fins and then a blunted 0.040-inch-thick stainless-steel overlay covered the leading edge of the inconel cap. The fins of the third stage had a cant angle of approximately $1^{\circ}$ each ($3^{\circ}51'$ total angle) to provide the necessary spin for stabilization of the velocity package after separation from the third stage (approximately 10 cycles per second). The third-stage fins were also alined with the first- and second-stage fins. Fin misalinements for all stages were held to an angle of less than $0^{\circ}10'$ for each fin.

A separation mechanism attached to the front of the third stage provided the means of detaching the velocity package from the third stage. A schematic drawing of the operation of this separation mechanism is shown in reference 1. The four-channel performance telemeter was housed in the separation-mechanism section to monitor the vehicle performance through separation of the third stage and the velocity package.

## Velocity Package

A sketch of the velocity package, which housed the rearward firing fourth, fifth, sixth, and seventh stages is shown in figure 3. The nose of the velocity package was a hemispherical segment tangent to an $8^{\circ}$ half-angle cone frustum. Another cone frustum of approximately $2^{\circ}$ half-angle formed the tube section of the velocity package which in turn faired into a cylinder. The arrangement of the rocket motors in the velocity package is also shown in figure 3. The fourth-stage T40 rocket motor was inserted into the velocity package and held in place on the guide rails by means of a blowout diaphragm threaded to the torque nozzle and similar to the diaphragm described for the second stage. The fourth-stage T40 rocket motor had a special torque nozzle which imparted an additional spin rate of approximately 20 cycles per second to the already existing 10 cycles per second from the third-stage fins for spin stabilization of the last two stages. The fifth-stage T55 rocket motor, the sixth-stage 5-inch spherical motor, and the seventh-stage shaped-charge accelerator were cantilevered from the fourth stage. Small hollow-column gauze-coated phenolic stiffeners were glued to the inside of the velocity package and at the juncture of the fifth and sixth stages within the velocity package to aid in supporting the inner structure.

Before the vehicle was assembled for launch, several combinations of components were dynamically balanced. The various combinations balanced were (1) the fifth, sixth, and seventh stages, (2) the fourth, fifth, sixth, and seventh stages, and (3) the velocity package complete with inner structure. Weights were added to each combination until the principal axis inclination was less than $0.02^{\circ}$ for the fifth, sixth, and seventh stages and less than $0.01^{\circ}$ for the velocity package with the internal stages. Photographs of several combinations of components on the dynamic balancing machine are shown in figure 21.

## REFERENCES


1. McCrosky, Richard E., and Soberman, Robert K.: Results From an Artificial Iron Meteoroid at 10 km/sec. AFCRL-62-803, U.S. Air Force, July 1962.

2. Gardner, William N., Brown, Clarence A., Jr., Henning, Allen B., Hook, W. Ray, Lundstrom, Reginald R., and Ramsey, Ira W., Jr.: Description of Vehicle System and Flight Tests of Nine Trailblazer I Reentry Physics Research Vehicles. NASA TN D-2189, 1964.

3. Gregory, Donald T., and Carraway, Ausley B.: Investigation of the Static Longitudinal Stability and Roll Characteristics of a Three-Stage Missile Configuration at Mach Numbers From 1.77 to 2.87. NASA TM X-124, 1959.

4. Robinson, Ross B.: Effects of Body and Fin Deflections on the Aerodynamic Characteristics in Pitch of a 0.065-Scale Model of a Four-Stage Rocket Configuration at Mach Numbers of 1.41 and 1.82. NASA TN D-37, 1959.

5. Henning, Allen B., Lundstrom, Reginald R., and Keating, Jean C.: A Wind-Compensation Method and Results of Its Application to Flight Tests of Twelve Trailblazer Rocket Vehicles. NASA TN D-2053, 1964.

6. Jewell, W. O., and Wineman, A. R.: Preliminary Analysis of a Simulated Meteor Reentry at 9.8 Kilometers Per Second. NASA TN D-2268, 1964.

7. Kemp, N. H., and Riddell, F. R.: Heat Transfer to Satellite Vehicles Re-entering the Atmosphere. Res. Rep. 2, AVCO Res. Lab., Oct. 1956. (Formerly Res. Note 21.)

TABLE I.- WEIGHT BREAKDOWN OF TRAILBLAZER Ig

| | Weight, lb |
|---|---|
| Seventh stage: | |
| Shaped-charge accelerator (276.5 grams) | 0.61 |
| Total this stage | 0.61 |
| Sixth stage: | |
| 5-inch motor case and liner | 0.30 |
| 5-inch propellant | 3.74 |
| Nozzle alone | 0.27 |
| Pellet in grain | 0.01 |
| 5-inch rocket motor loaded | 4.32 |
| Igniter assembly | 0.13 |
| Diaphragm | 0.04 |
| Total this stage | 4.49 |
| Total previous stages | 0.61 |
| Total including this stage | 5.10 |
| Fifth stage: | |
| Adaptor (5-inch motor to T55) section | 0.63 |
| Loaded T55 RM (nozzle, nose cap, and shroud) | 49.25 |
| Ears for sleeve | 0.31 |
| Igniter assembly | 0.69 |
| Balance | 0.16 |
| Total this stage | 51.04 |
| Total previous stages | 5.10 |
| Total including this stage | 56.14 |
| Fourth stage: | |
| T55 diaphragm | 0.56 |
| Adaptor (T40 to T55) | 1.37 |
| Loaded T40 with nozzle | 134.00 |
| Igniter assembly | 0.75 |
| Diaphragm (T40 to package) | 0.56 |
| Balance | 1.31 |
| Total this stage | 138.55 |
| Total previous stages | 56.14 |
| Total including this stage | 194.69 |

TABLE I.- WEIGHT BREAKDOWN OF TRAILBLAZER Ig - Continued

| | Weight, lb | |
|---|---|---|
| Velocity package skin: | | |
| Nose section | 13.50 | |
| Forward skin | 17.62 | |
| Rearward skin | 50.94 | |
| Timer | 2.56 | |
| Balance | 0.53 | |
| Total this stage | 85.15 | |
| Total previous stages | 194.69 | |
| Total including this stage | 279.84 | |
| Center of gravity, inches rearward of package nose | | 59.25 |
| Velocity package separation mechanism: | | |
| Separation mechanism | 75.90 | |
| Squib holder | 0.56 | |
| Timer assembly | 3.32 | |
| Total separation mechanism | 79.78 | |
| Total velocity package | 279.84 | |
| Total separation mechanism and velocity package | 359.62 | |
| Third-stage rocket motor: | | |
| TX77 rocket motor with 2-ft$^2$/panel fins, pyrogen unit, shroud, but no separation mechanism | 1,721.10 | |
| Initiators | 0.34 | |
| Total this stage | 1,721.44 | |
| Total previous stages | 359.62 | |
| Total including this stage | 2,081.06 | |
| Center of gravity, inches from thrust face of motor | | 85.45 |
| Second-stage rocket motor: | | |
| Nike rocket motor with $2\frac{1}{2}$ - ft$^2$/panel fins, adaptor, and flare holder | 1,297.00 | |
| Flares | 1.50 | |
| Igniter | 8.06 | |
| Total this stage | 1,306.56 | |
| Total previous stages | 2,081.06 | |
| Total including this stage | 3,387.62 | |
| Center of gravity, inches from thrust face | | 60.75 |

TABLE I.- WEIGHT BREAKDOWN OF TRAILBLAZER Ig - Concluded

| | Weight, lb | |
|---|---|---|
| First-stage rocket motor: | | |
| Honest John rocket motor with $7\frac{1}{2}$-$ft^2$/panel fins, adaptor, spin motors, and housing | 4,237.50 | |
| Igniter | 9.69 | |
| Total this stage | 4,247.19 | |
| Total previous stages | 3,387.62 | |
| Total including this stage | 7,634.81 | |
| Center of gravity, inches from thrust face | | 87.25 |
| Total of Trailblazer Ig at take-off | 7,634.81 | |

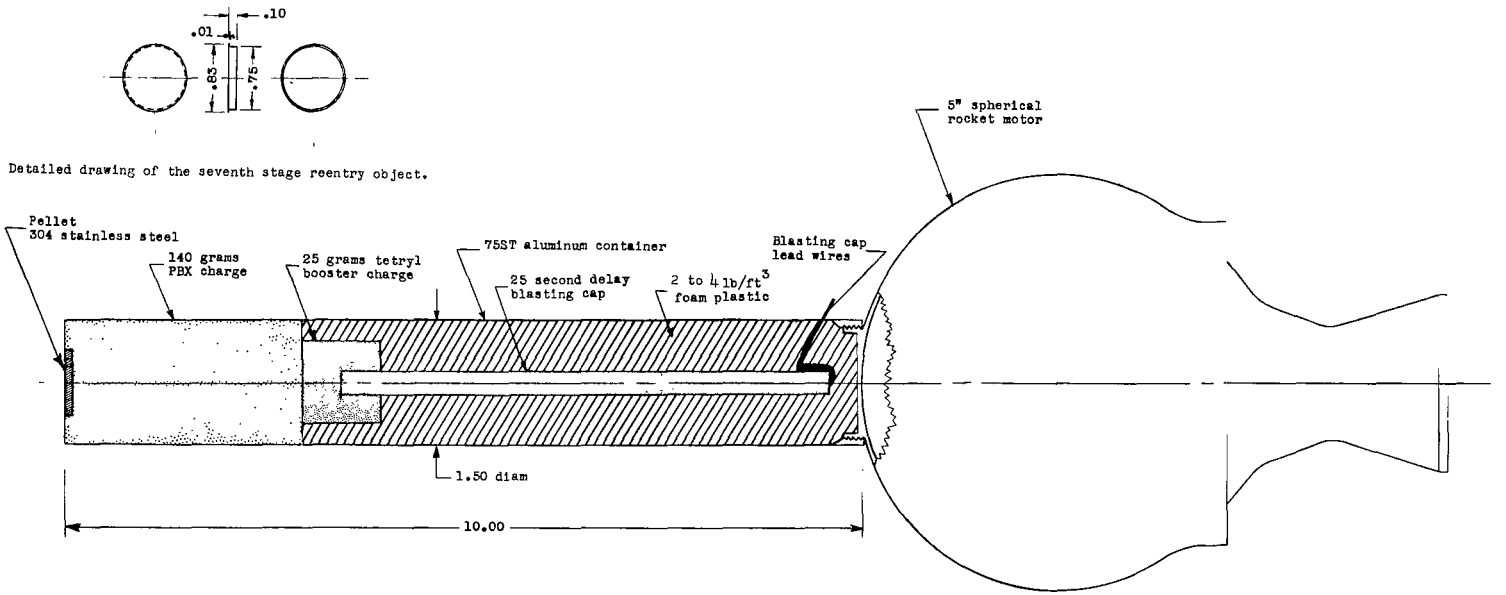


(a) Sketch of sixth and seventh stages and seventh-stage reentry object.

Figure 1.- Sixth and seventh stages of the Trailblazer Ig. Dimensions are in inches.

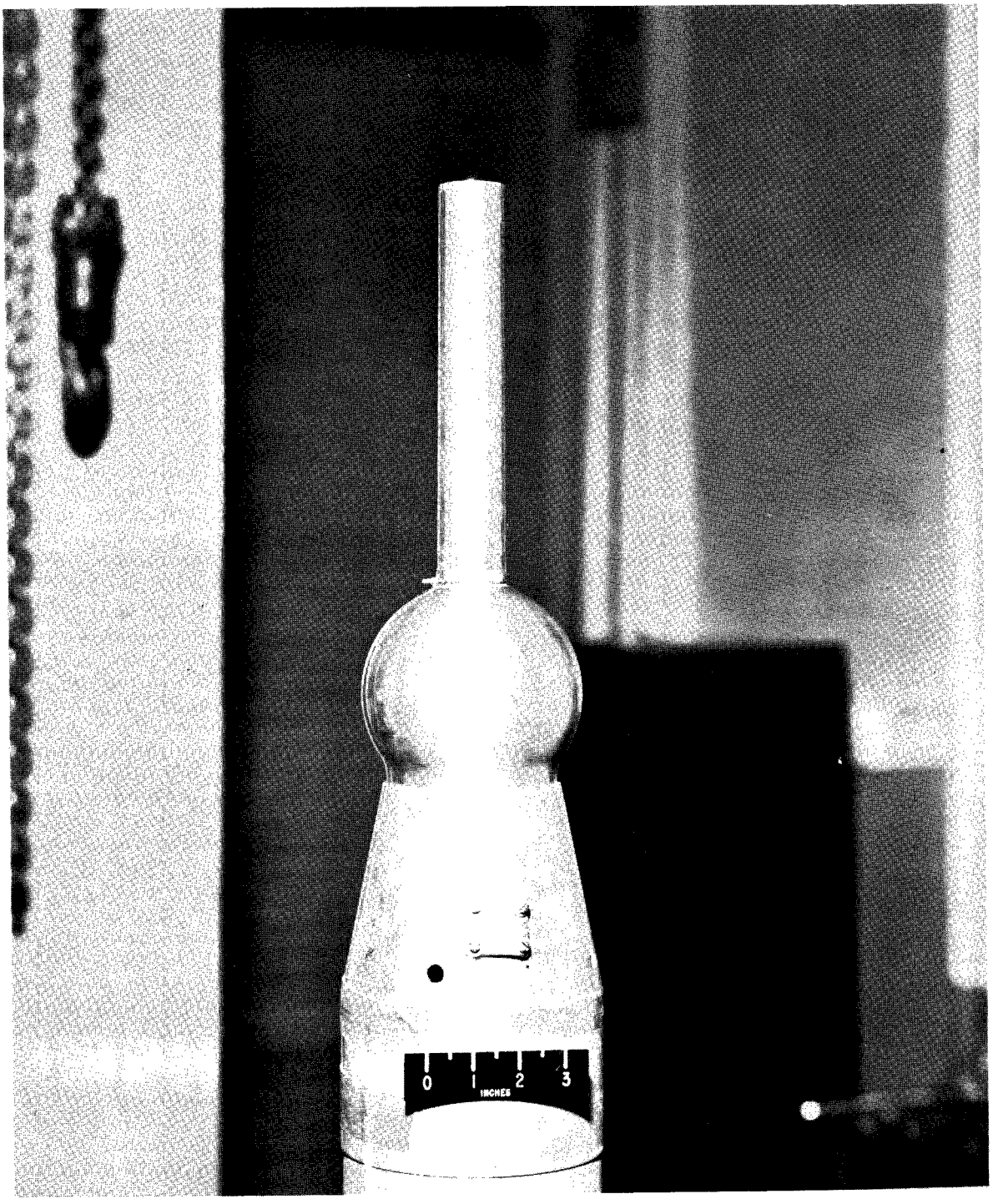


(b) Photograph of sixth and seventh stages. L-61-3077

Figure 1.- Concluded.

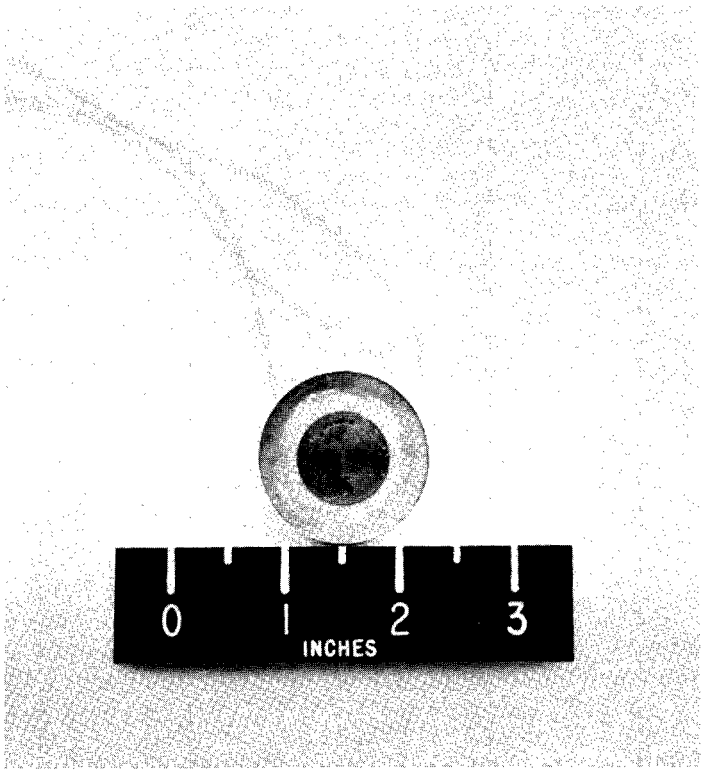


(a) End view of accelerator and pellet.

Figure 2.- Photograph of shaped-charge accelerator. L-61-3079

(b) Side view of accelerator. L-61-3080

Figure 2.- Concluded.

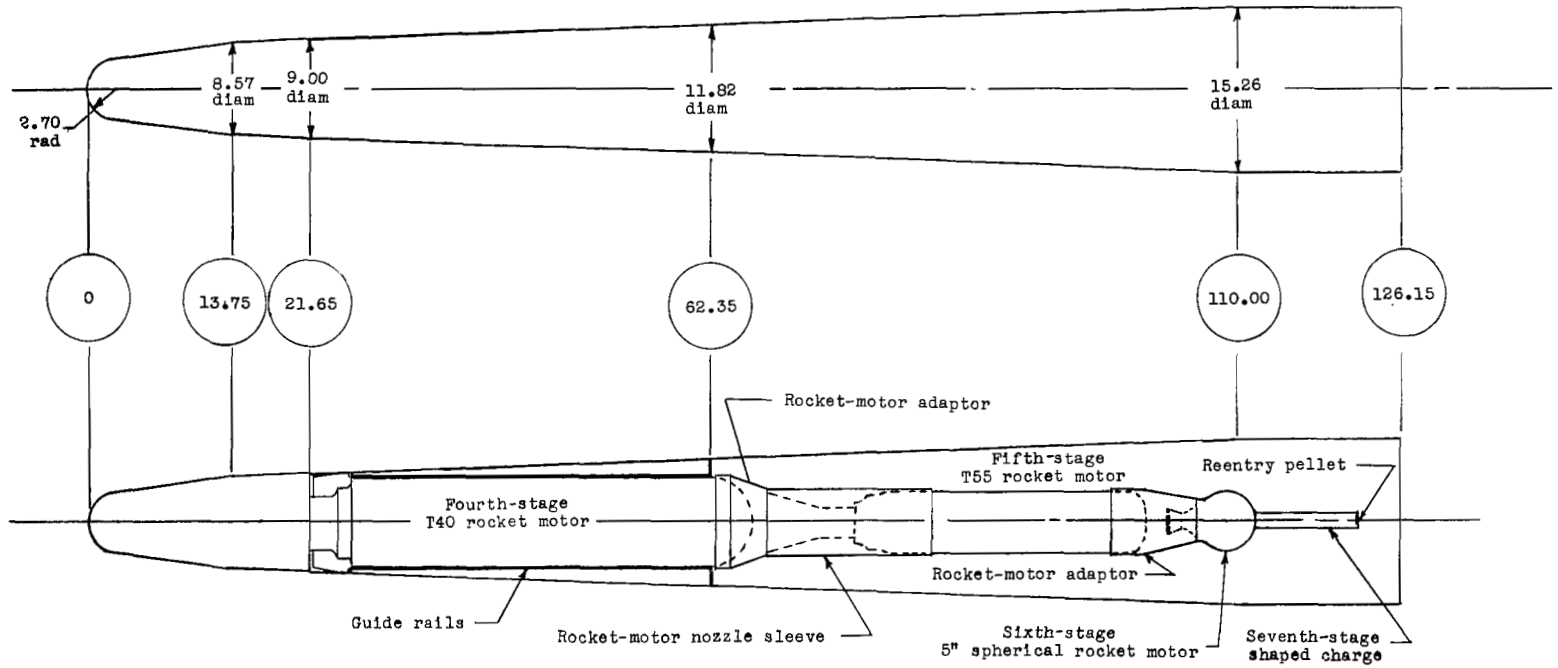


Figure 3.- Sketch of velocity package. All dimensions and station locations are in inches.

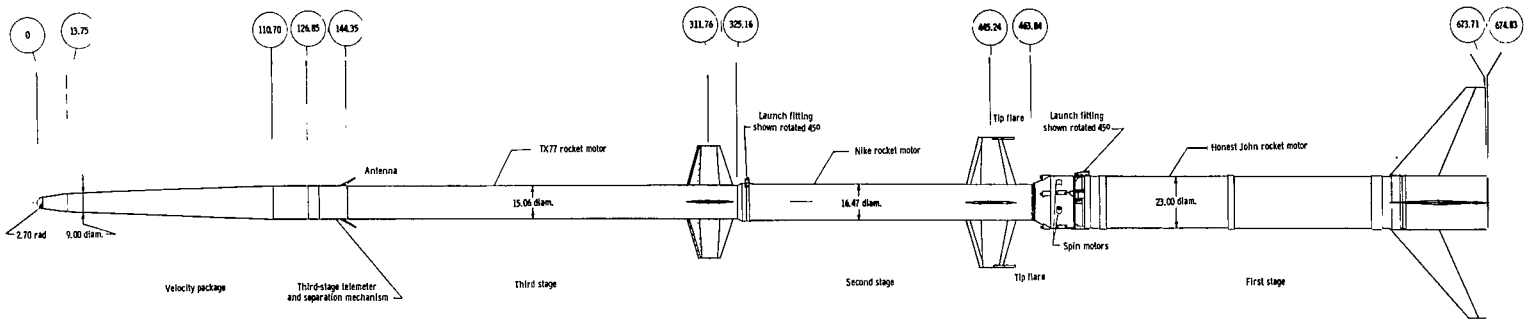


Figure 4.- Sketch of vehicle. All dimensions and station numbers are in inches.

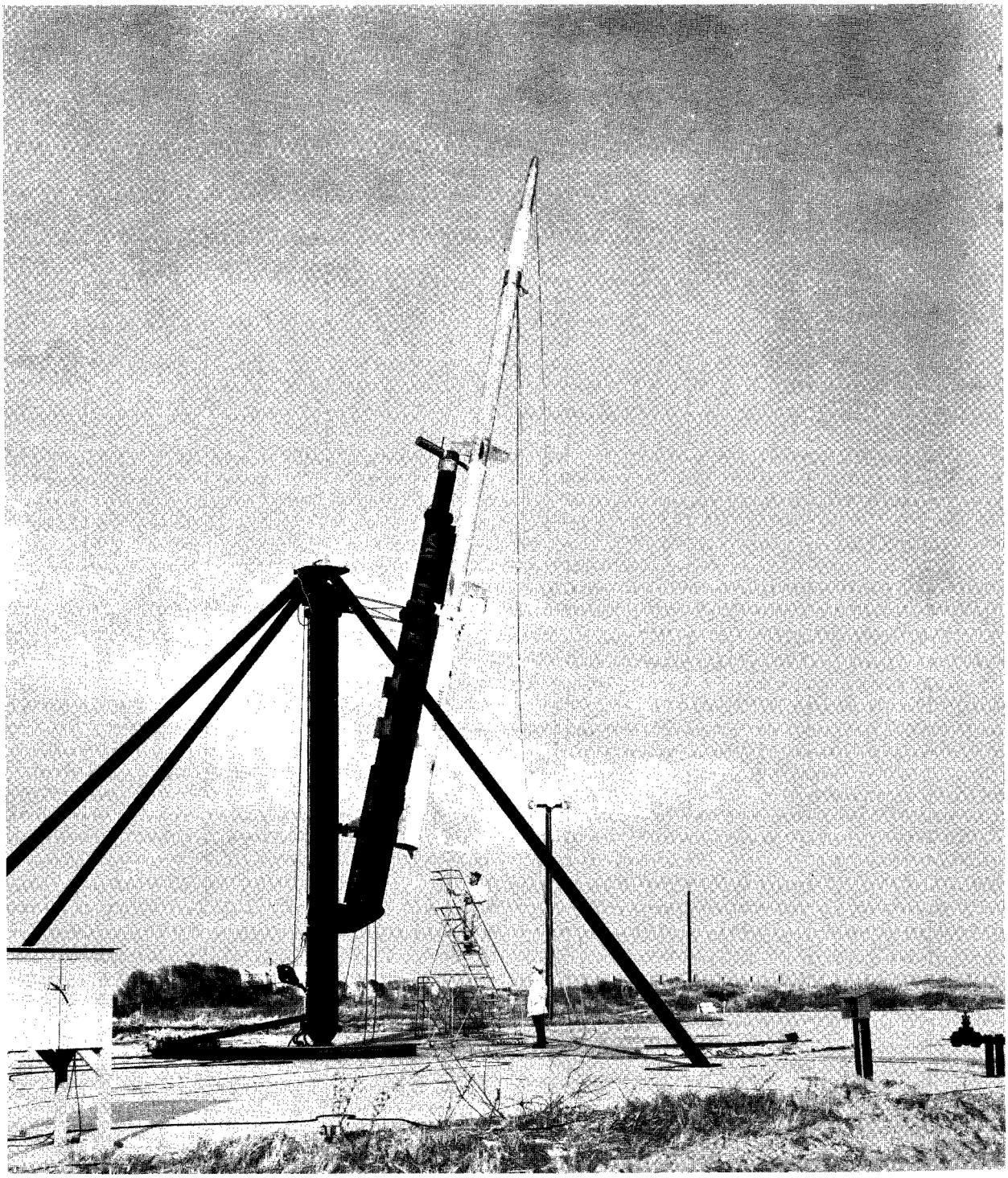

Figure 5.- Trailblazer Ig in launch position. L-61-3073

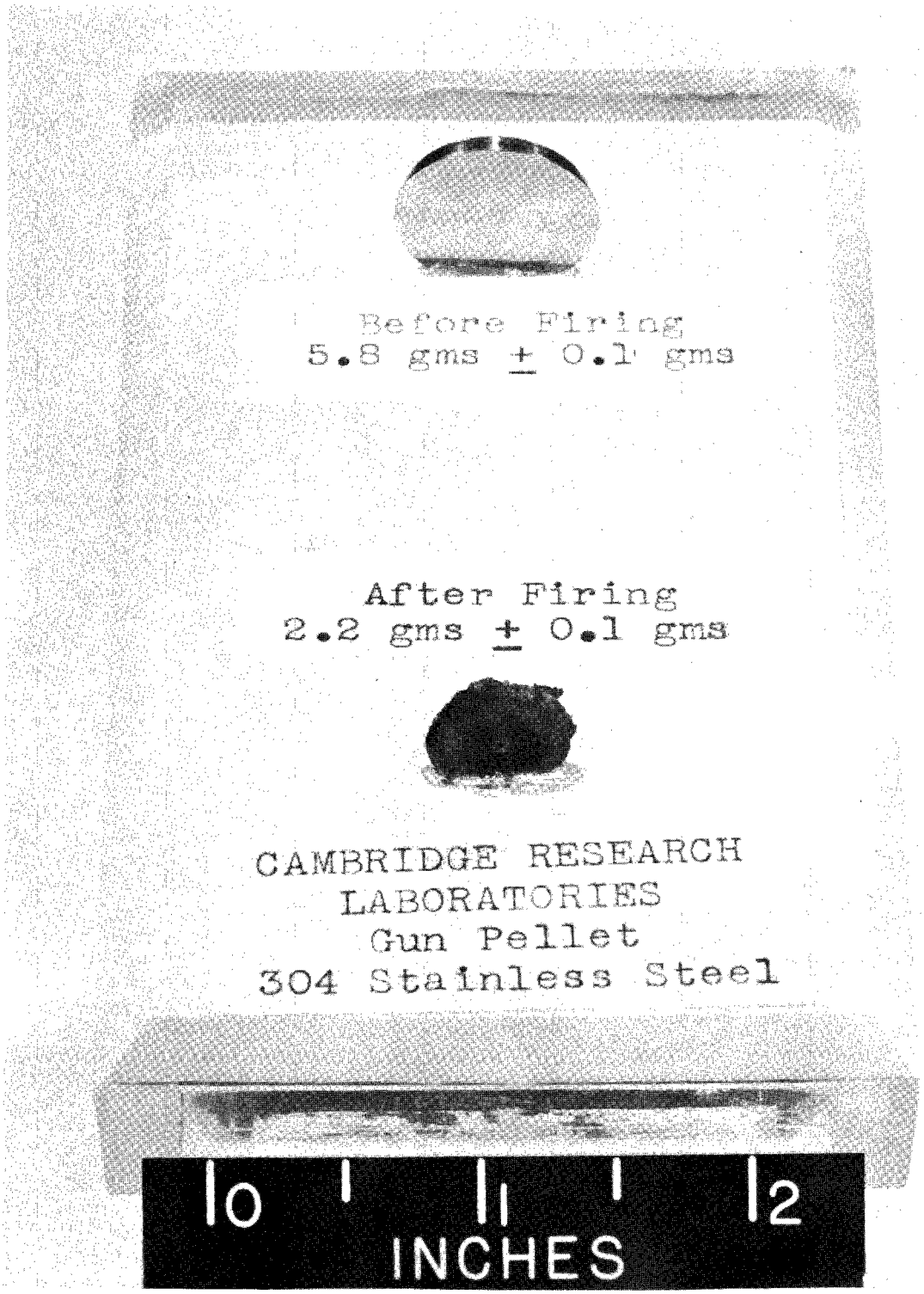


Figure 6.- Pellet before and after capture tests at Cambridge Research Laboratories. L-62-7818

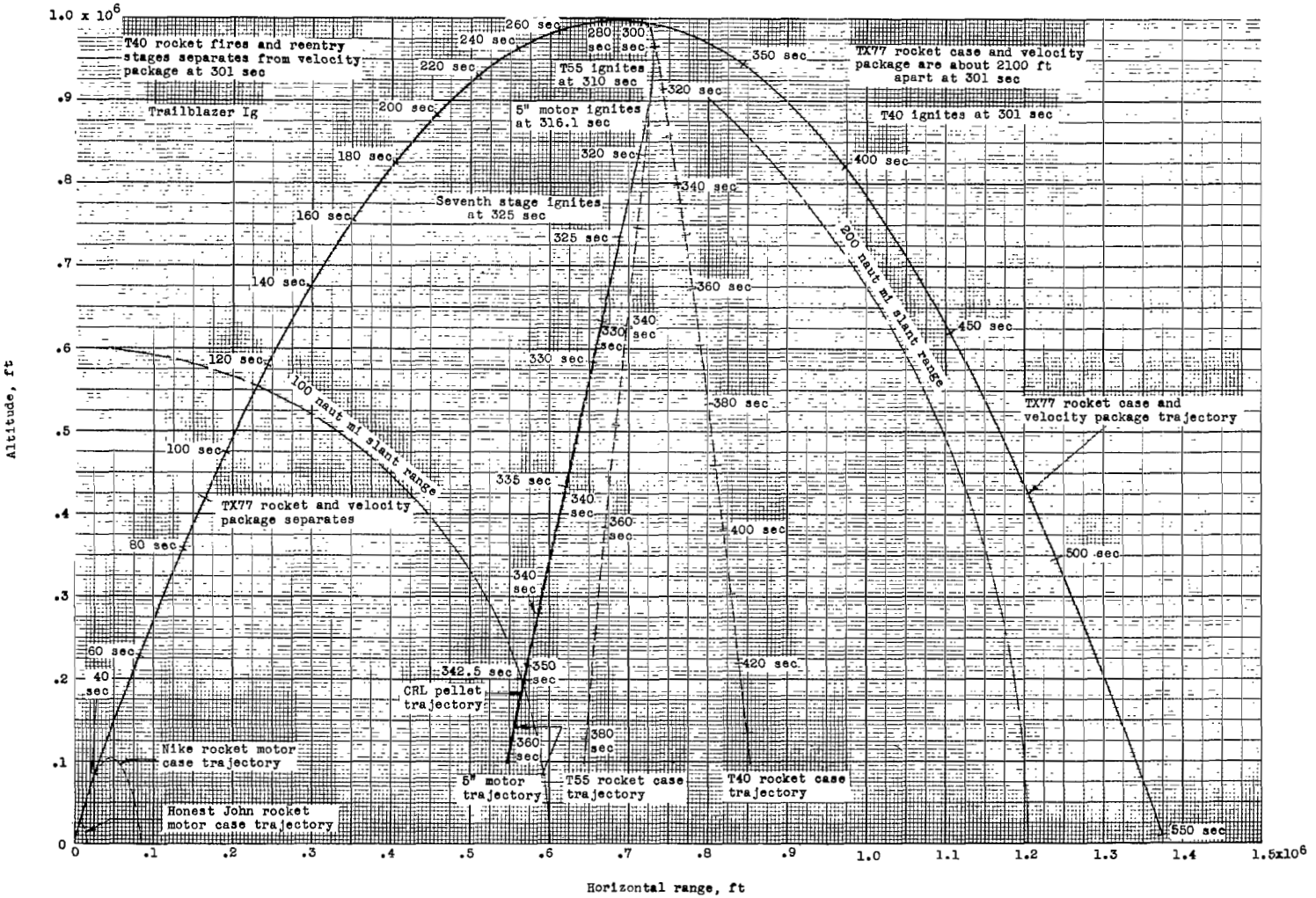


Figure 7.- Calculated trajectory for each stage at an 80° launch angle.

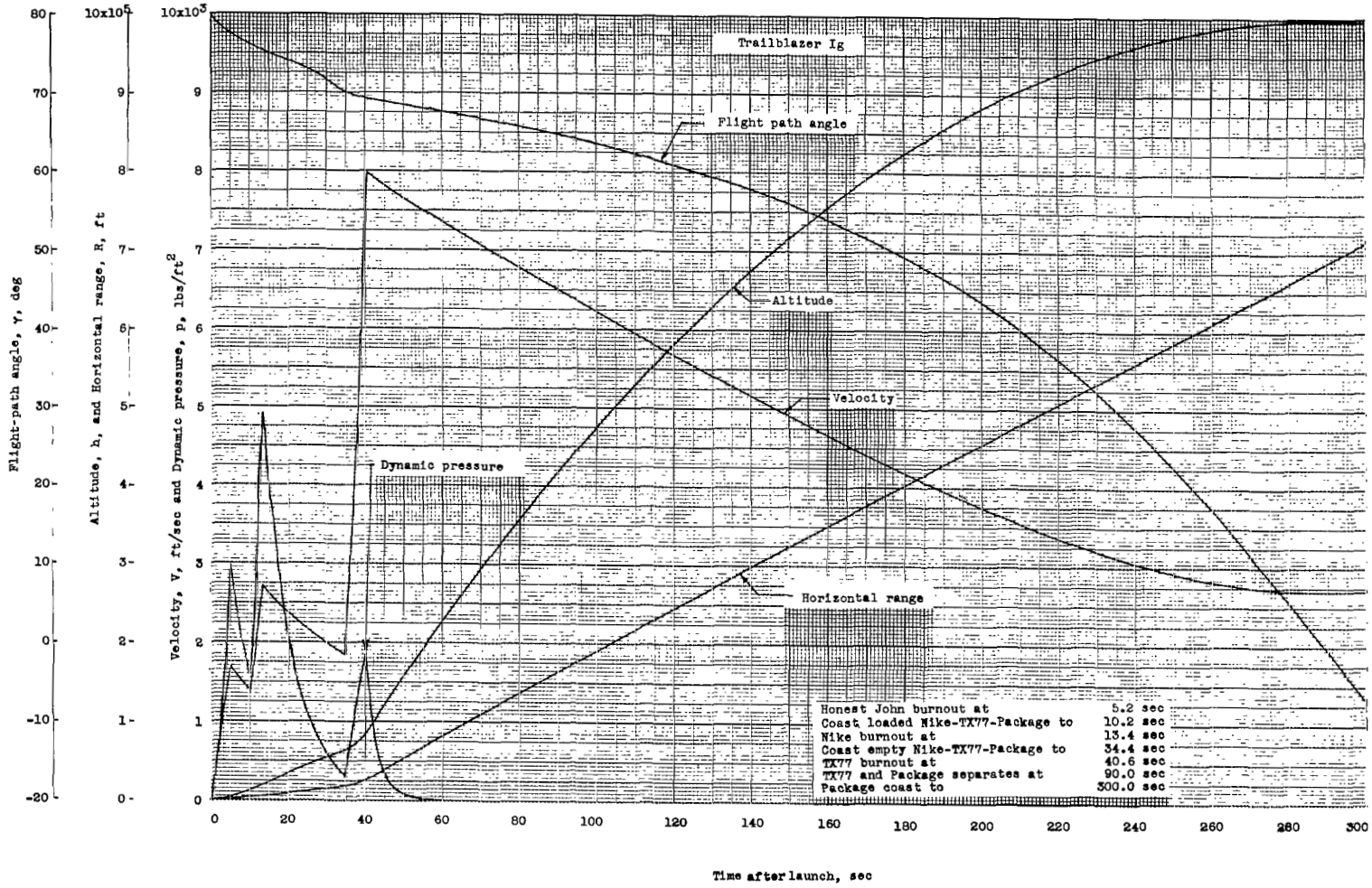


Figure 8.- Calculated time history for first 300 seconds of flight.

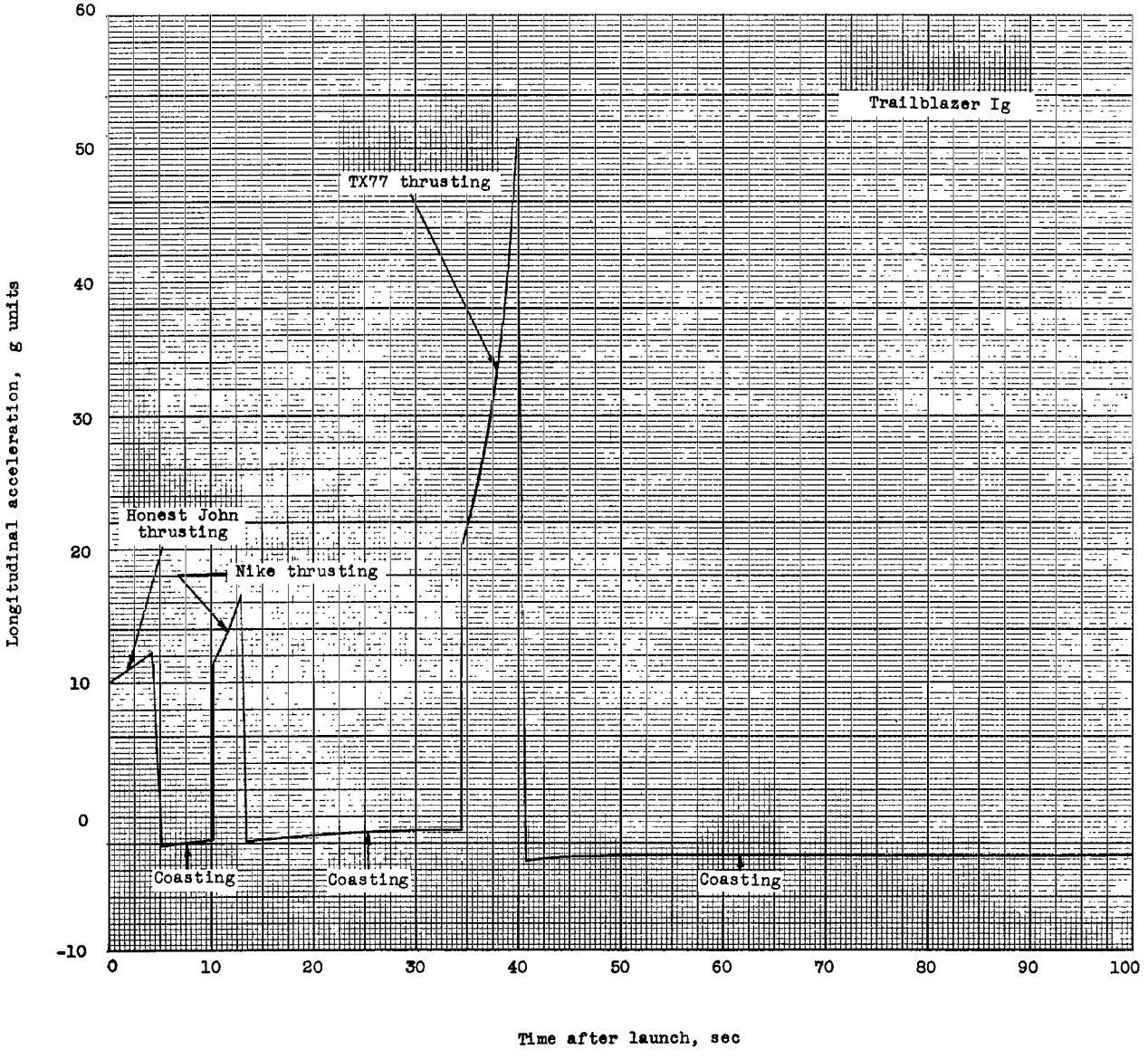


Figure 9.- Calculated longitudinal acceleration for first three stages.

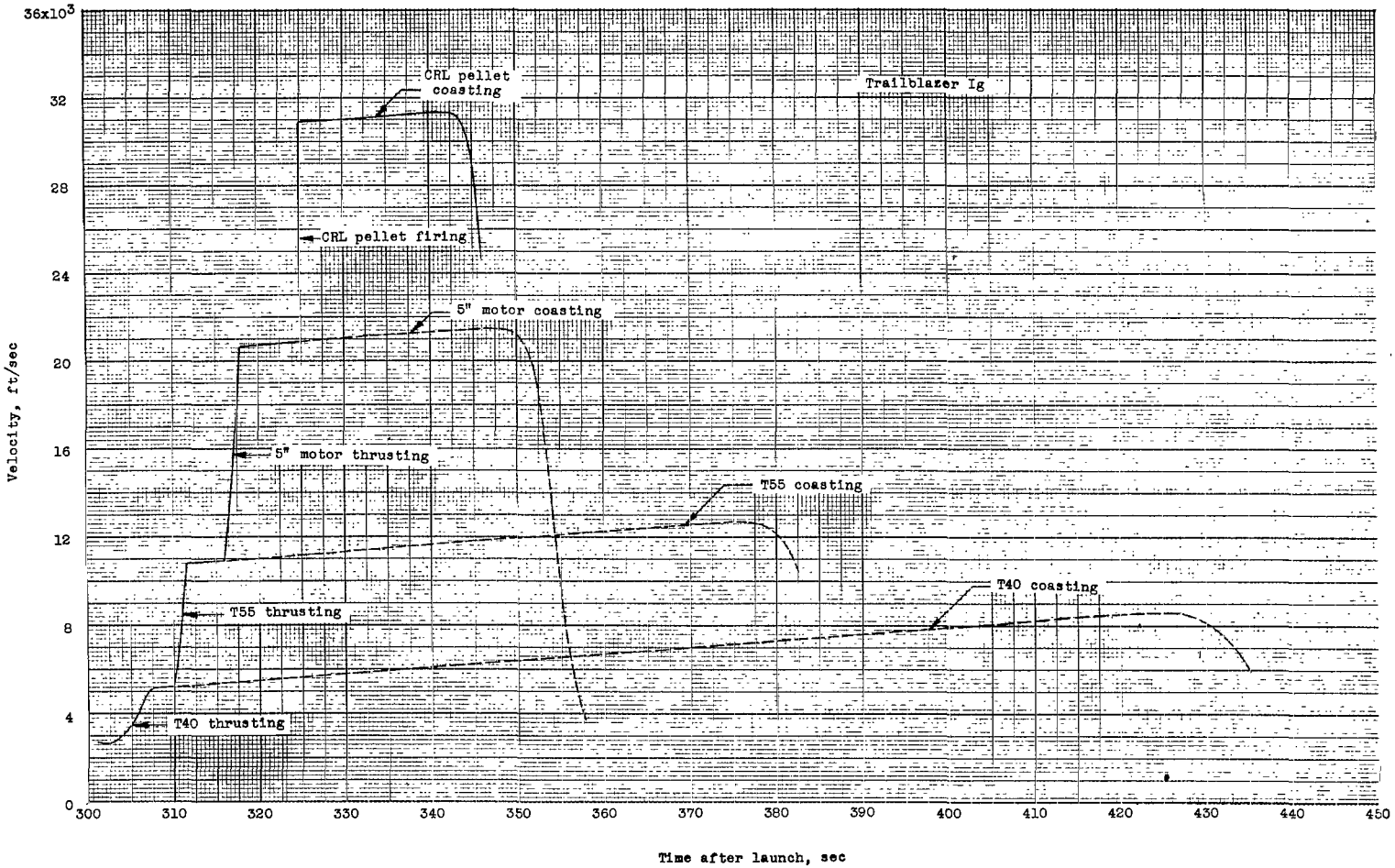


Figure 10.- Calculated velocity-time curves for reentering stages.

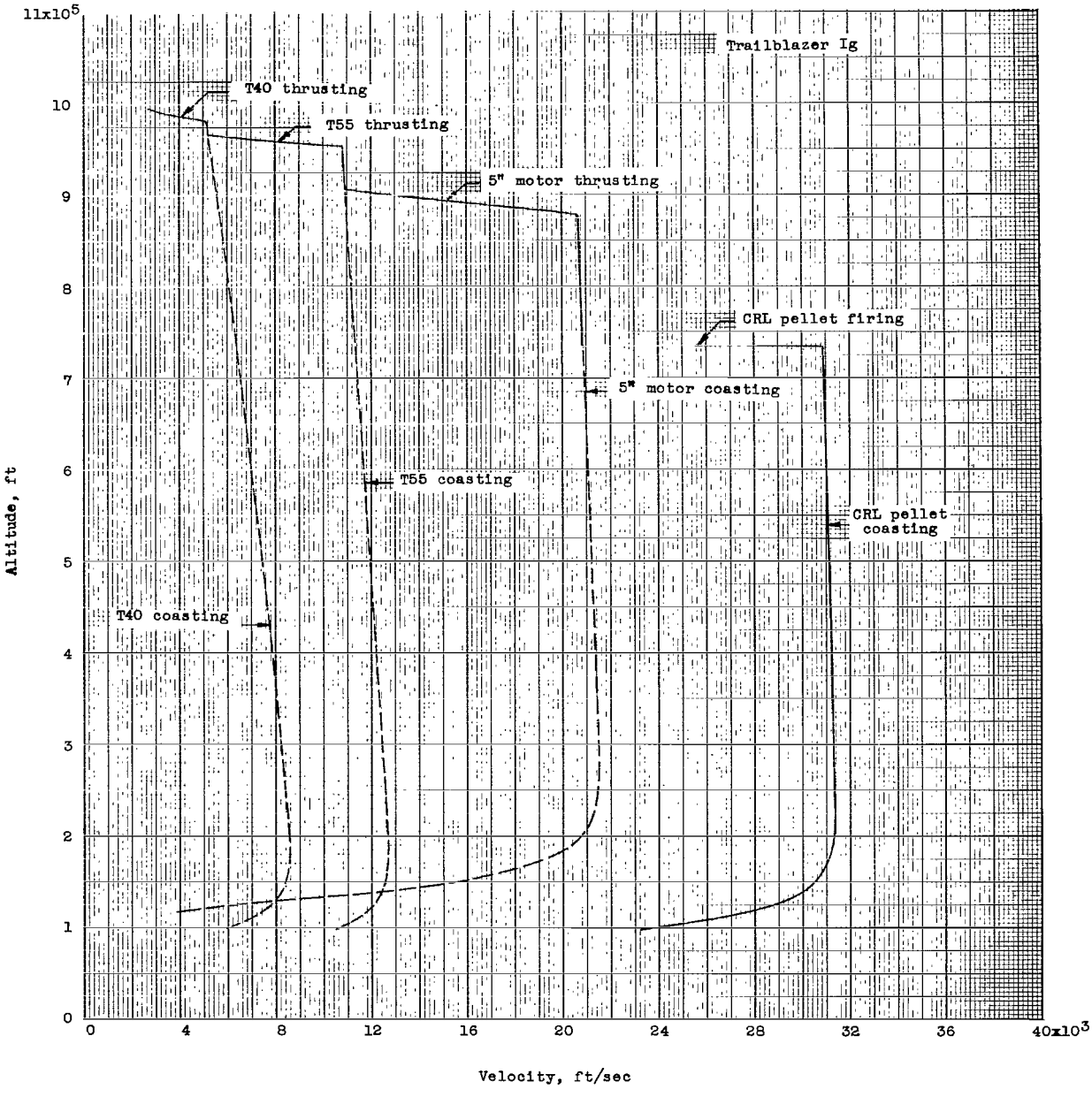


Figure 11.- Calculated velocity-altitude curves for reentering stages.

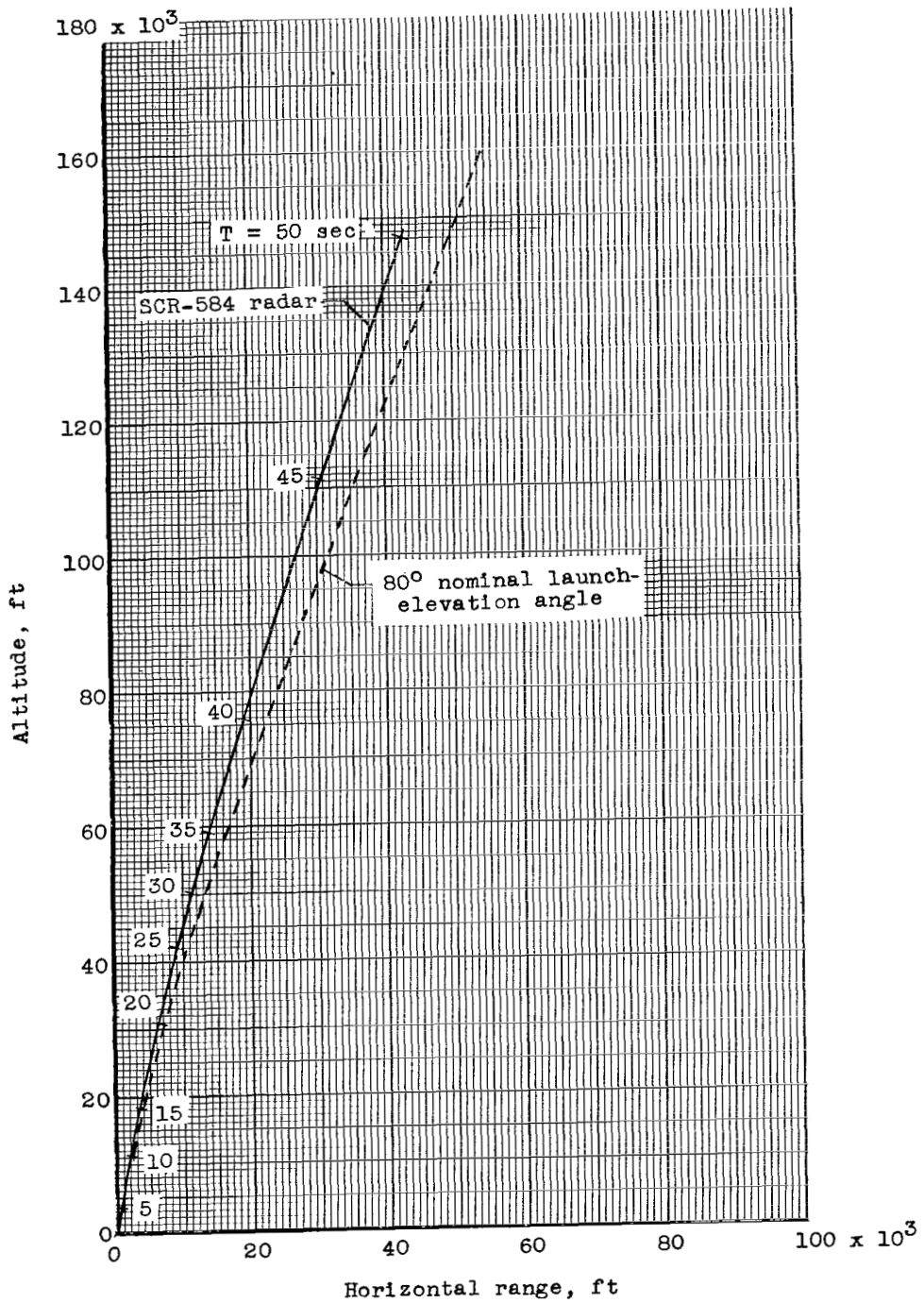


(a) Trajectory.

Figure 12.- Data obtained from SCR-584 radar.

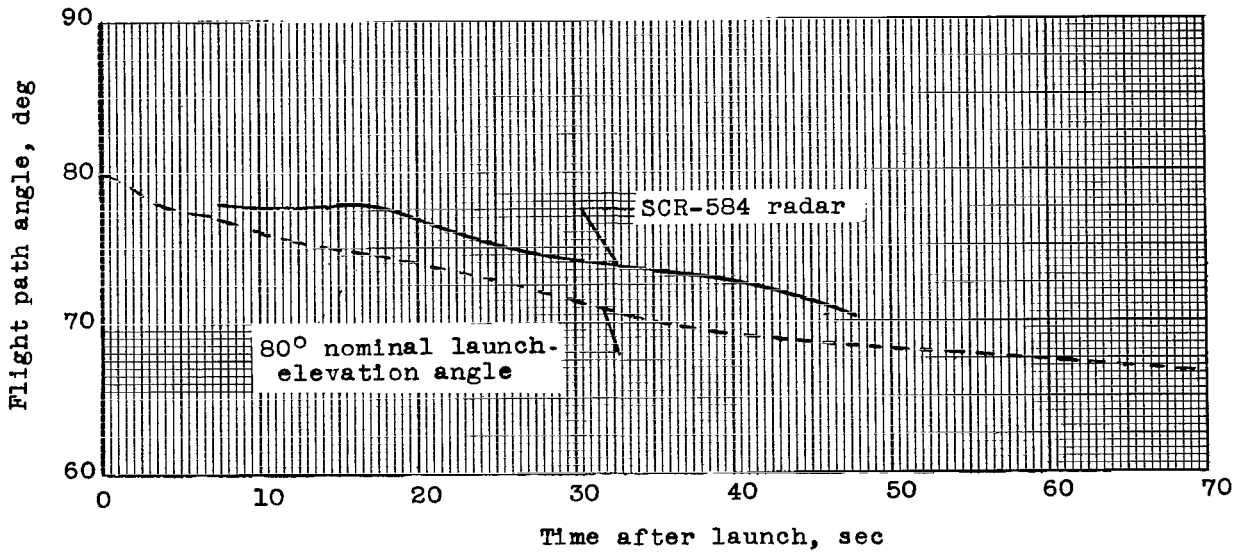


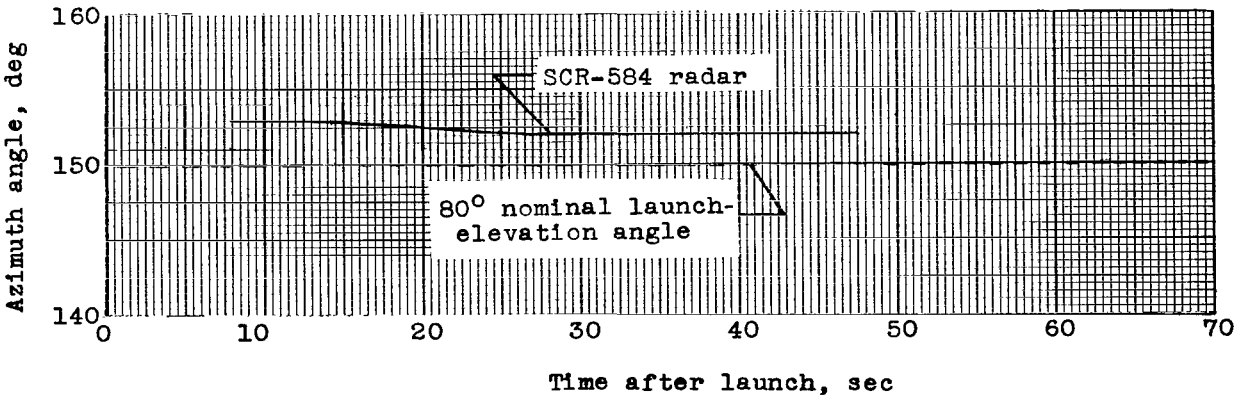


(b) Variation of flight-path angle and azimuth angle.

Figure 12.- Concluded.

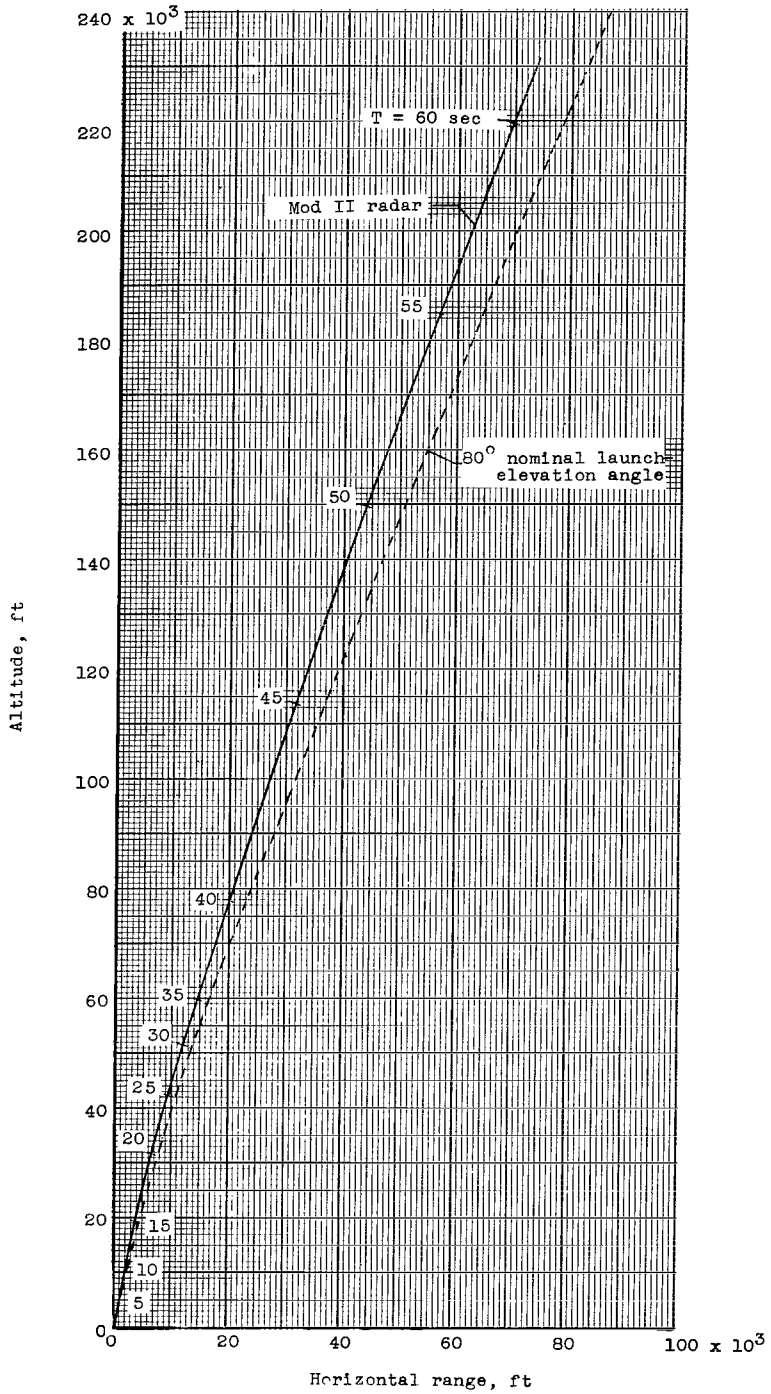


(a) Trajectory.

Figure 13.- Data obtained from Mod II radar.

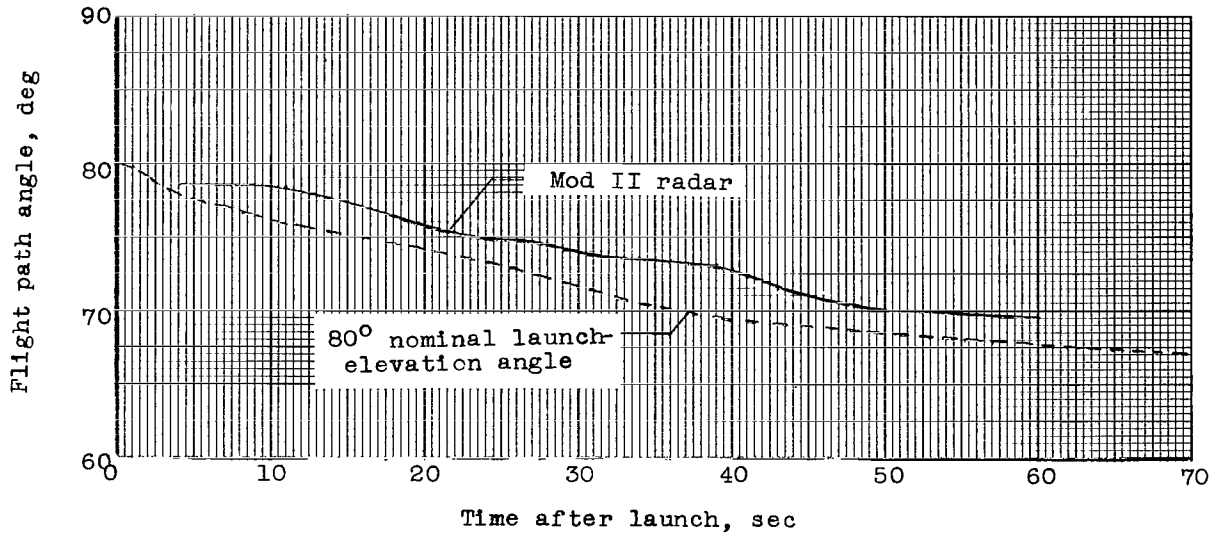


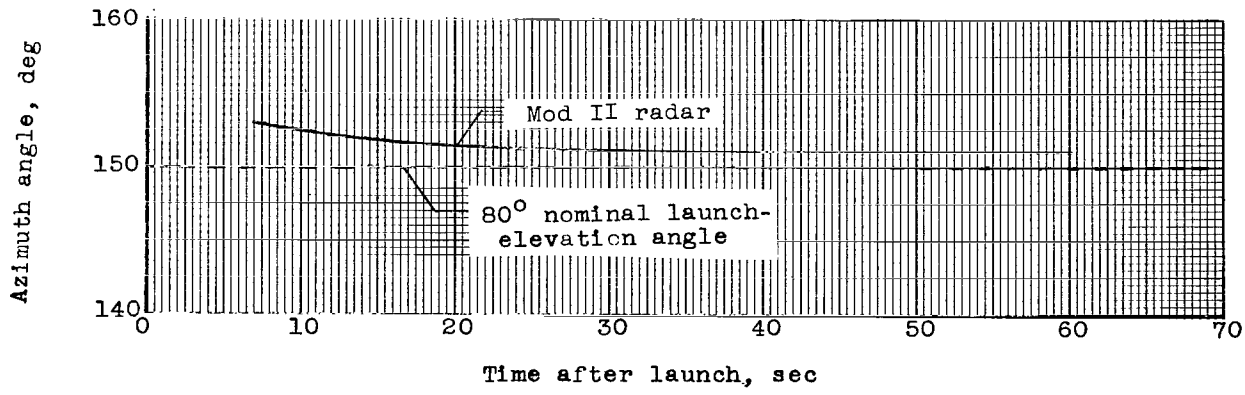


(b) Variation of flight-path angle and azimuth angle.

Figure 13.- Concluded.

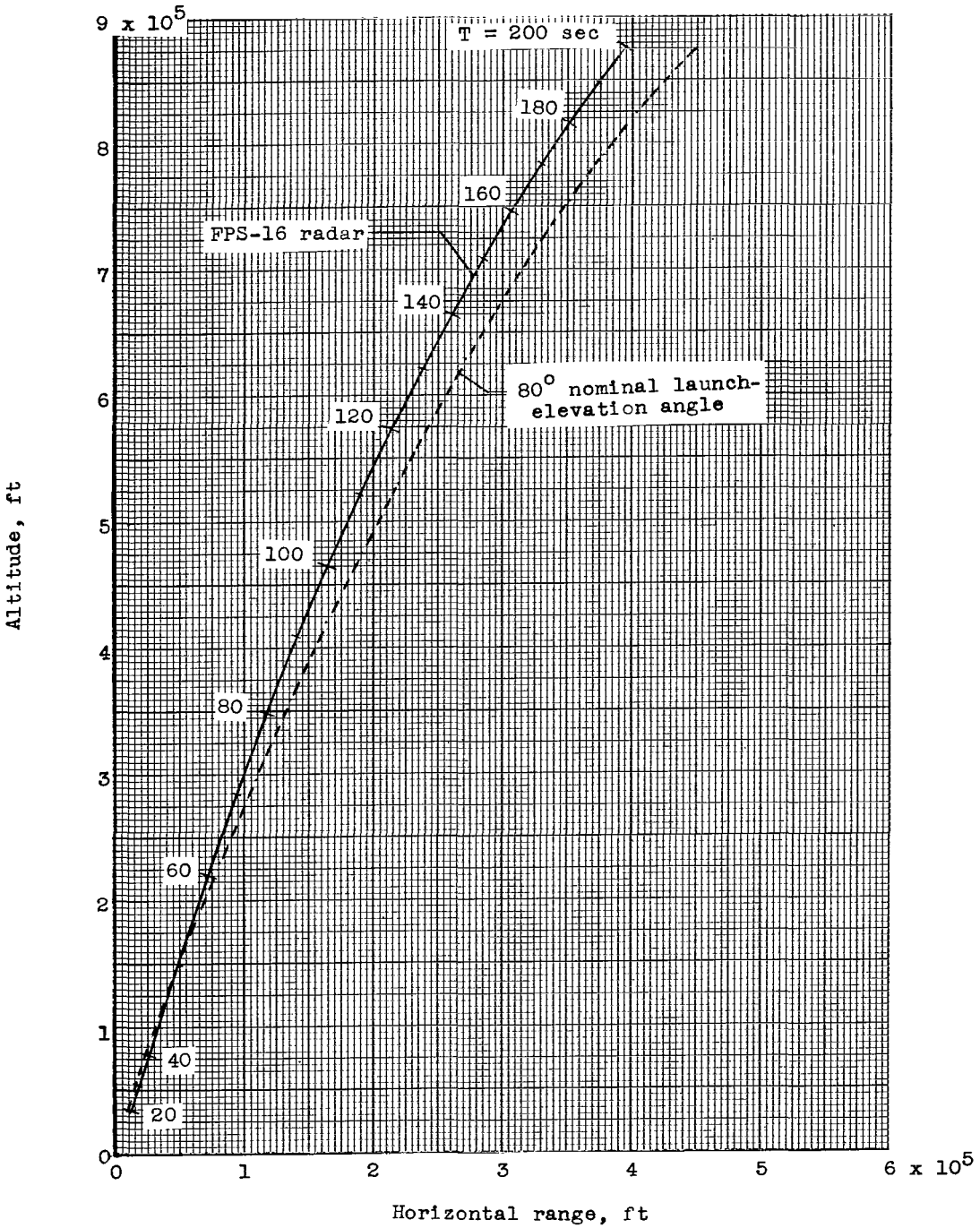


(a) Trajectory.

Figure 14.- Data obtained from FPS-16 radar.

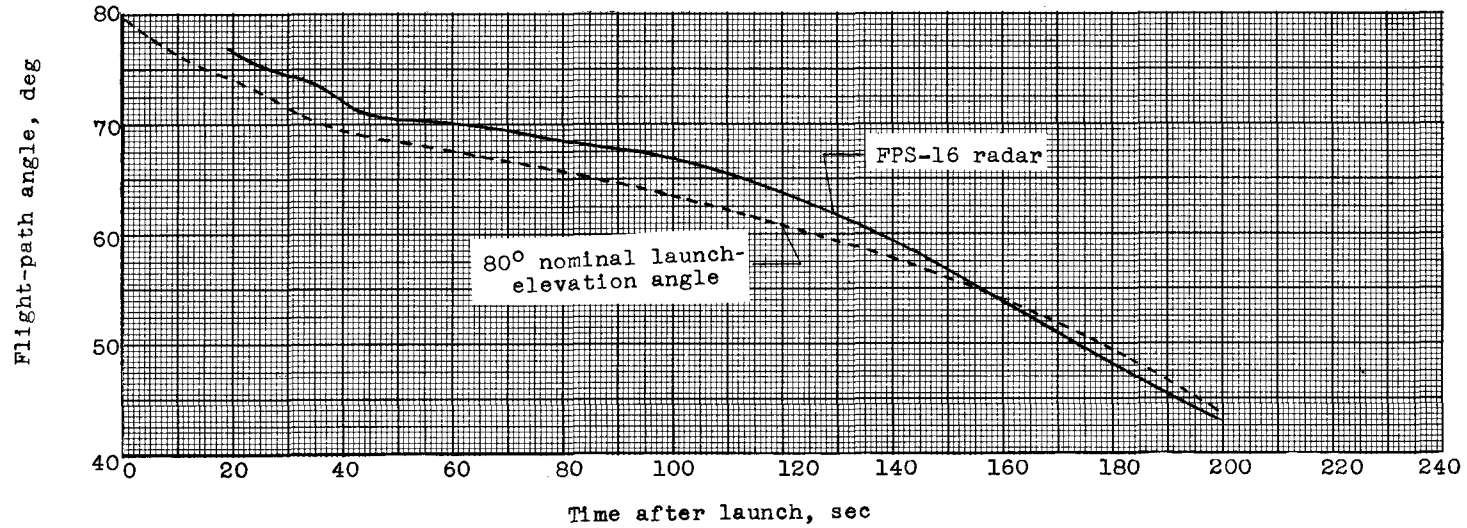


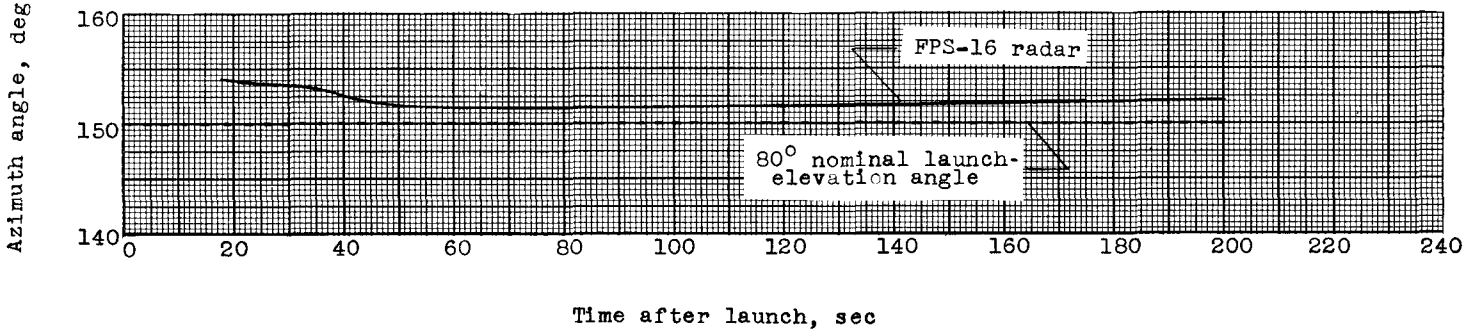


(b) Variation of flight-path angle and azimuth angle.

Figure 14.- Continued.

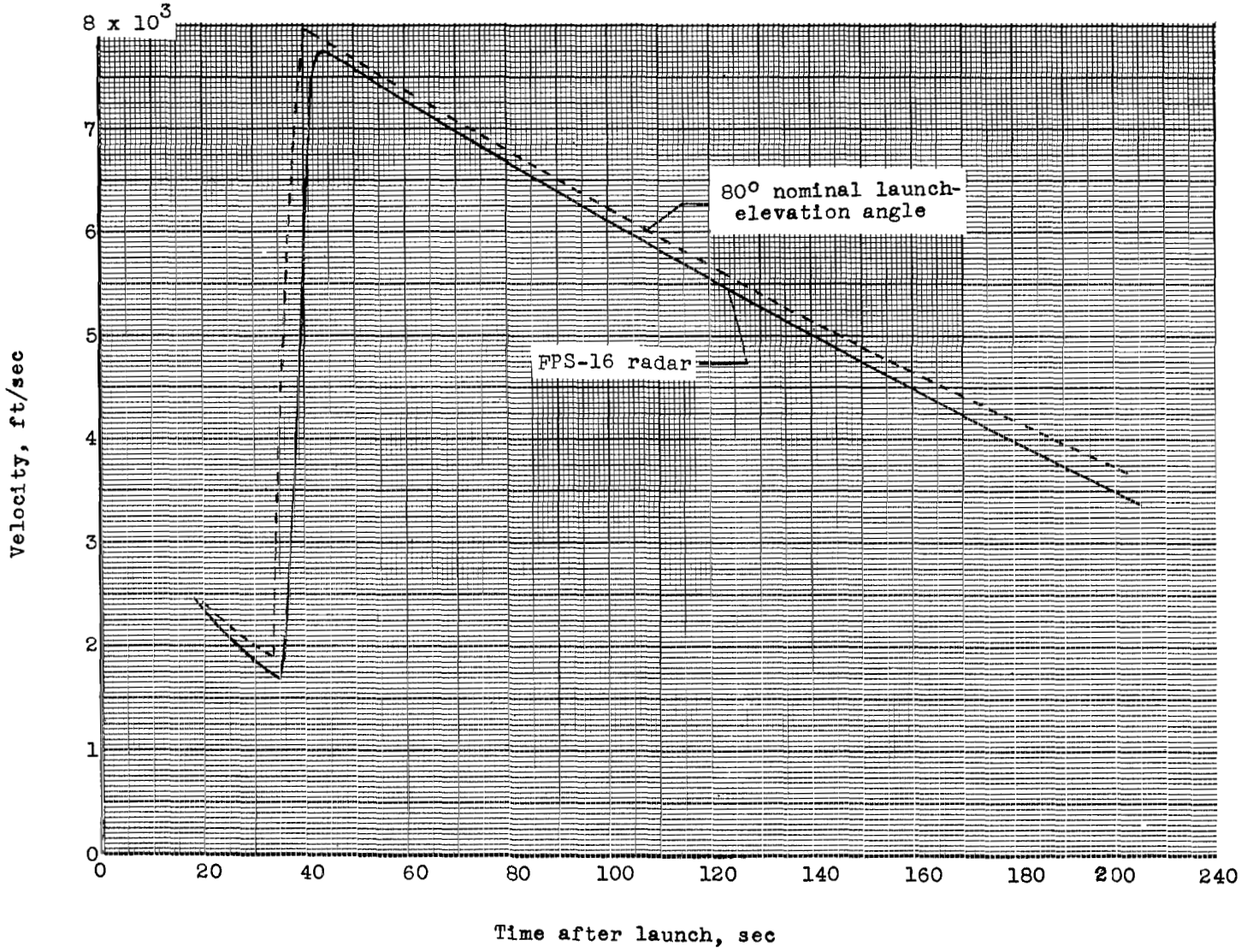


(c) Variation of velocity with time.

Figure 14.- Concluded.

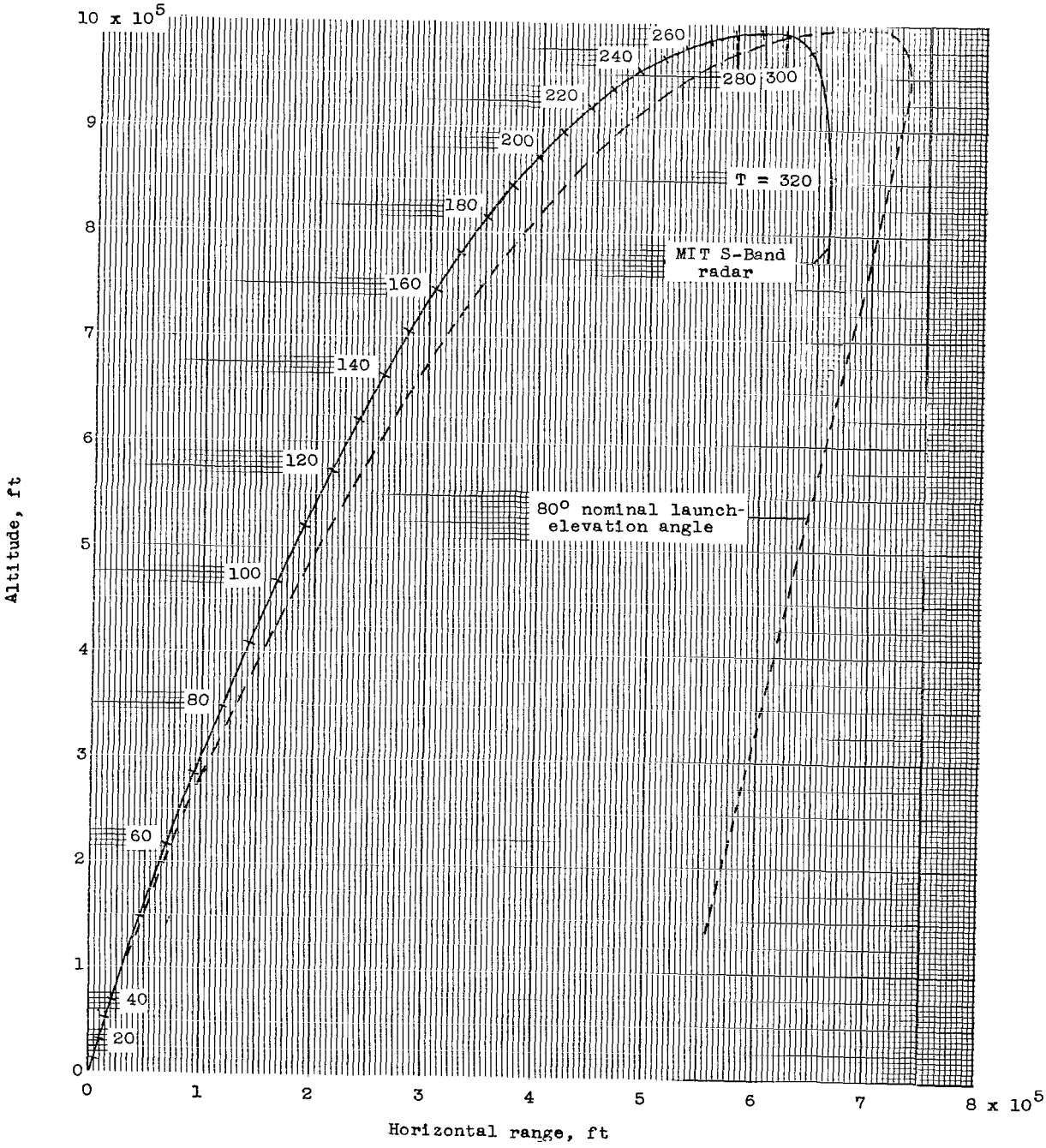


(a) Trajectory.

Figure 15.- Data obtained from MIT S-Band radar.

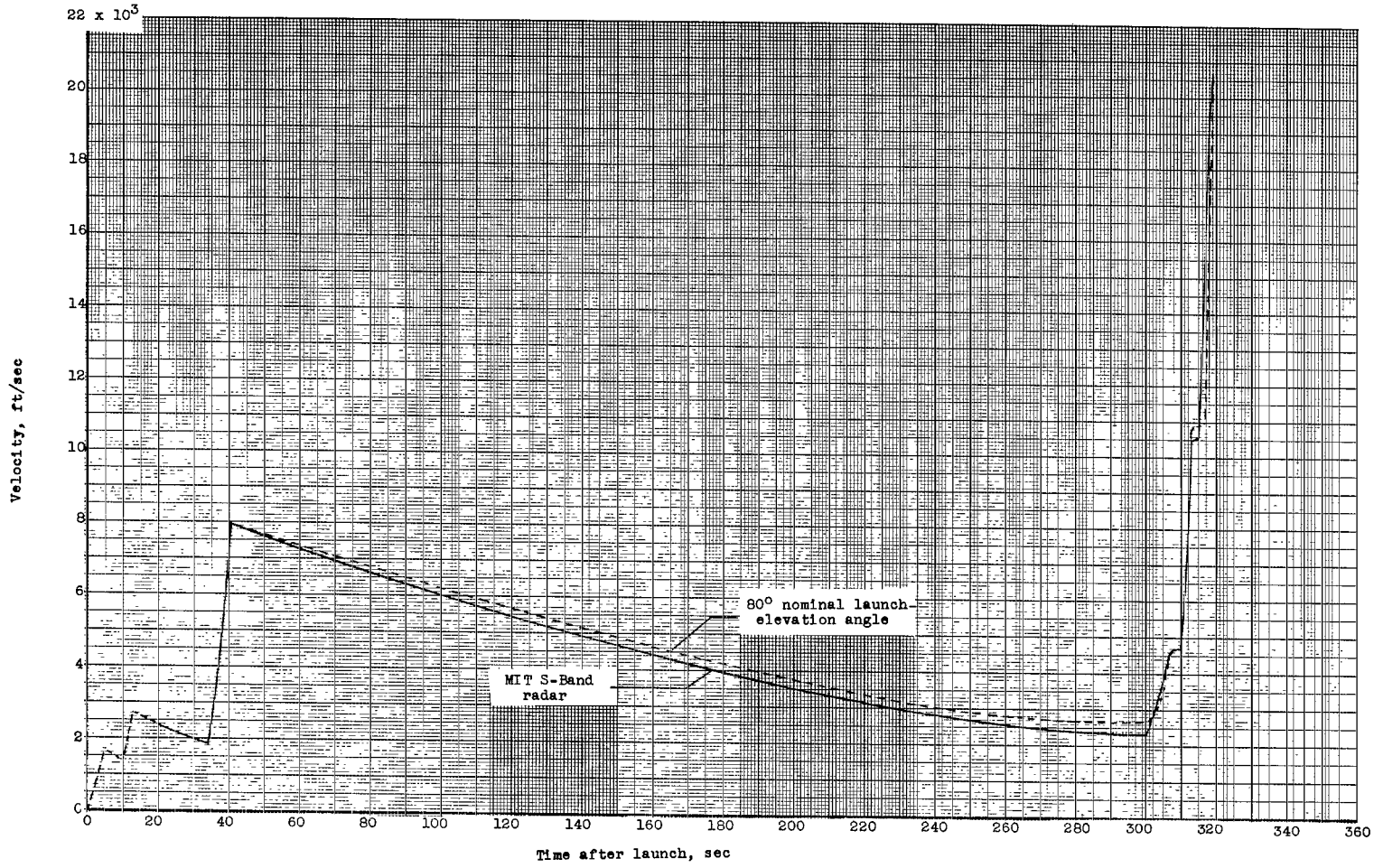


(b) Variation of velocity with time.

Figure 15.- Concluded.

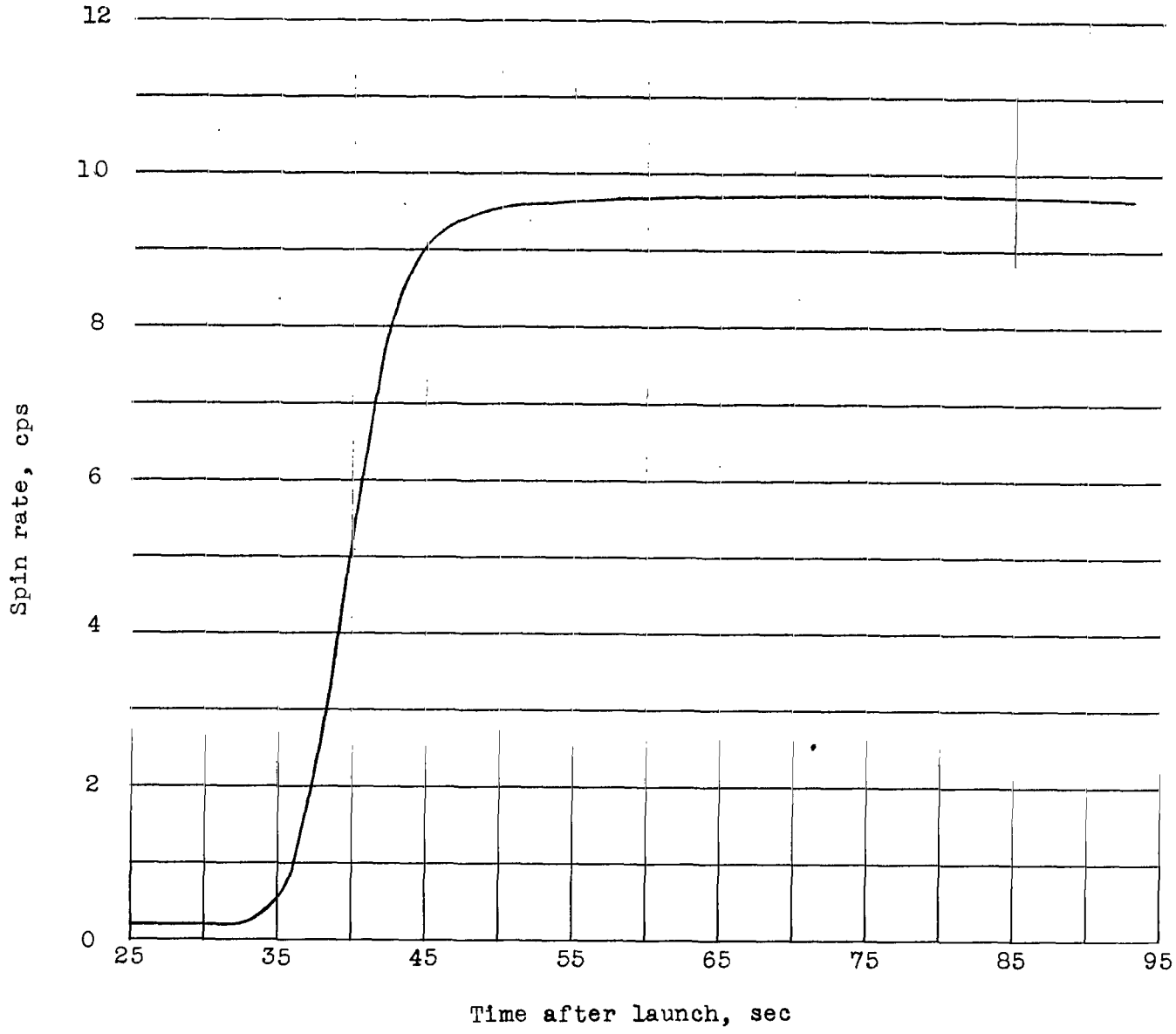


Figure 16.- Variation of spin rate (produced by third-stage fins) with time.

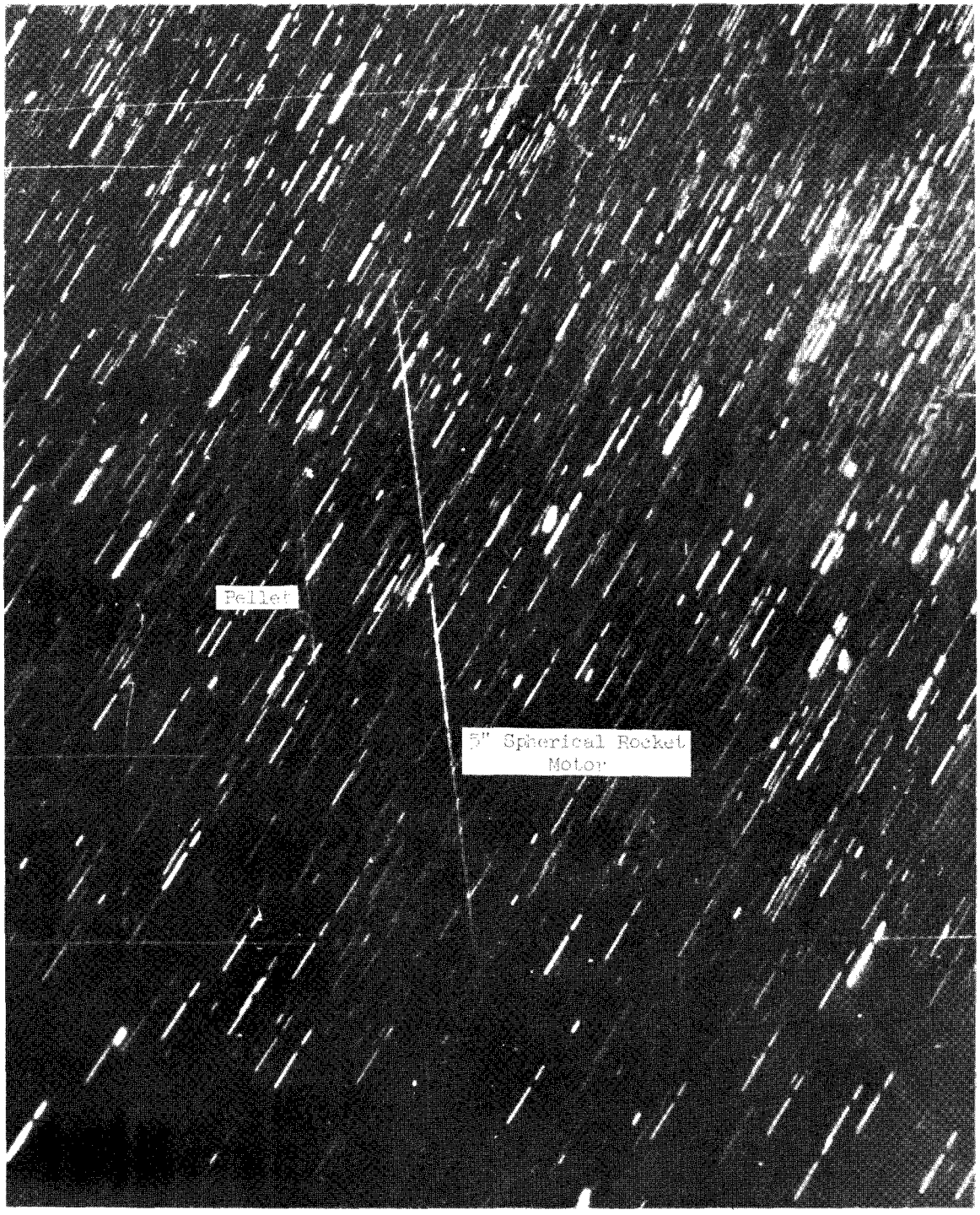


(a) Photograph of reentry of pellet and sixth stage.

Figure 17.- Reentry trail of Trailblazer Ig as viewed from Coquina Beach, N.C. tracking station. L-64-363

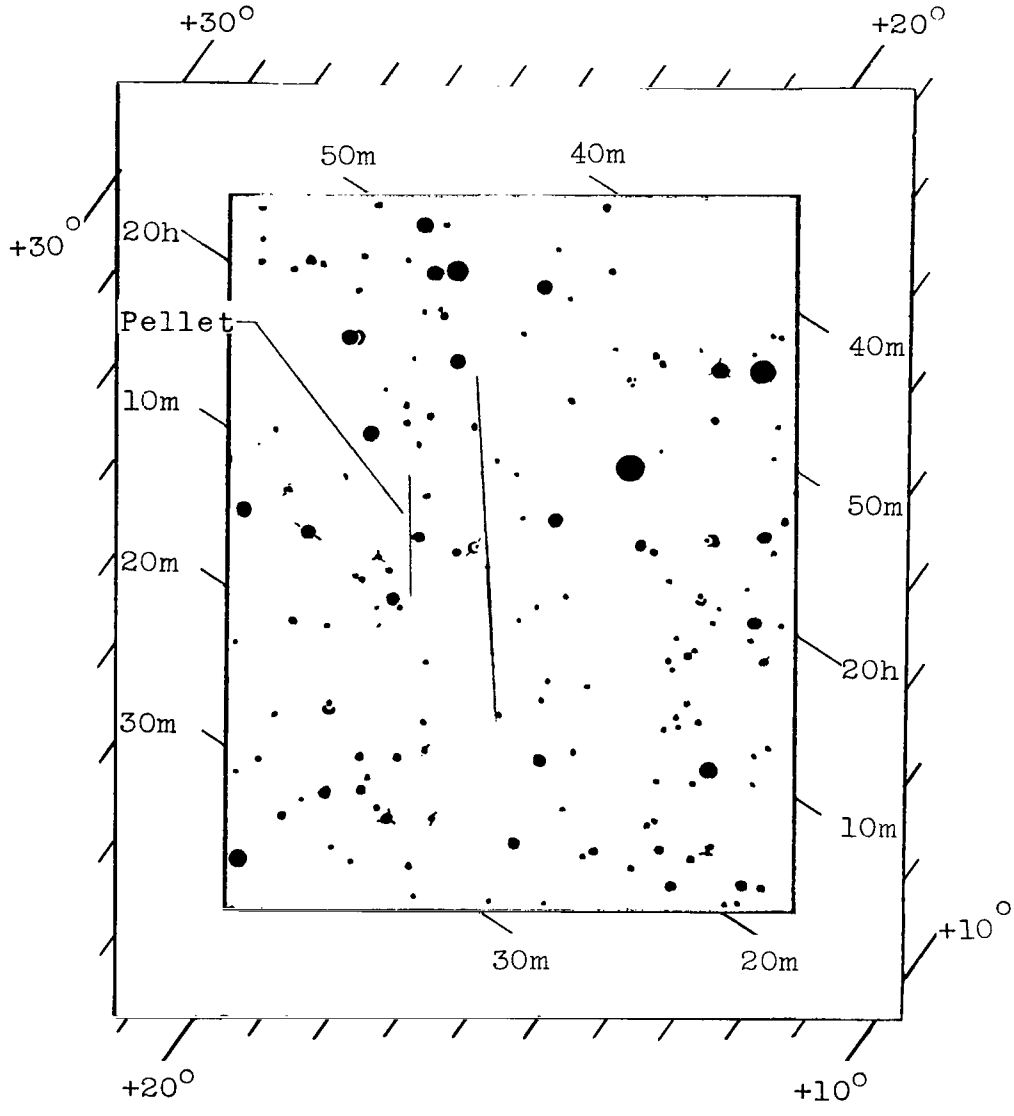


Note: Inner scale - right ascension, hr, min

Outer scale - declination, deg

(b) Sketch of the star background and reentry trail.

Figure 17.- Concluded.

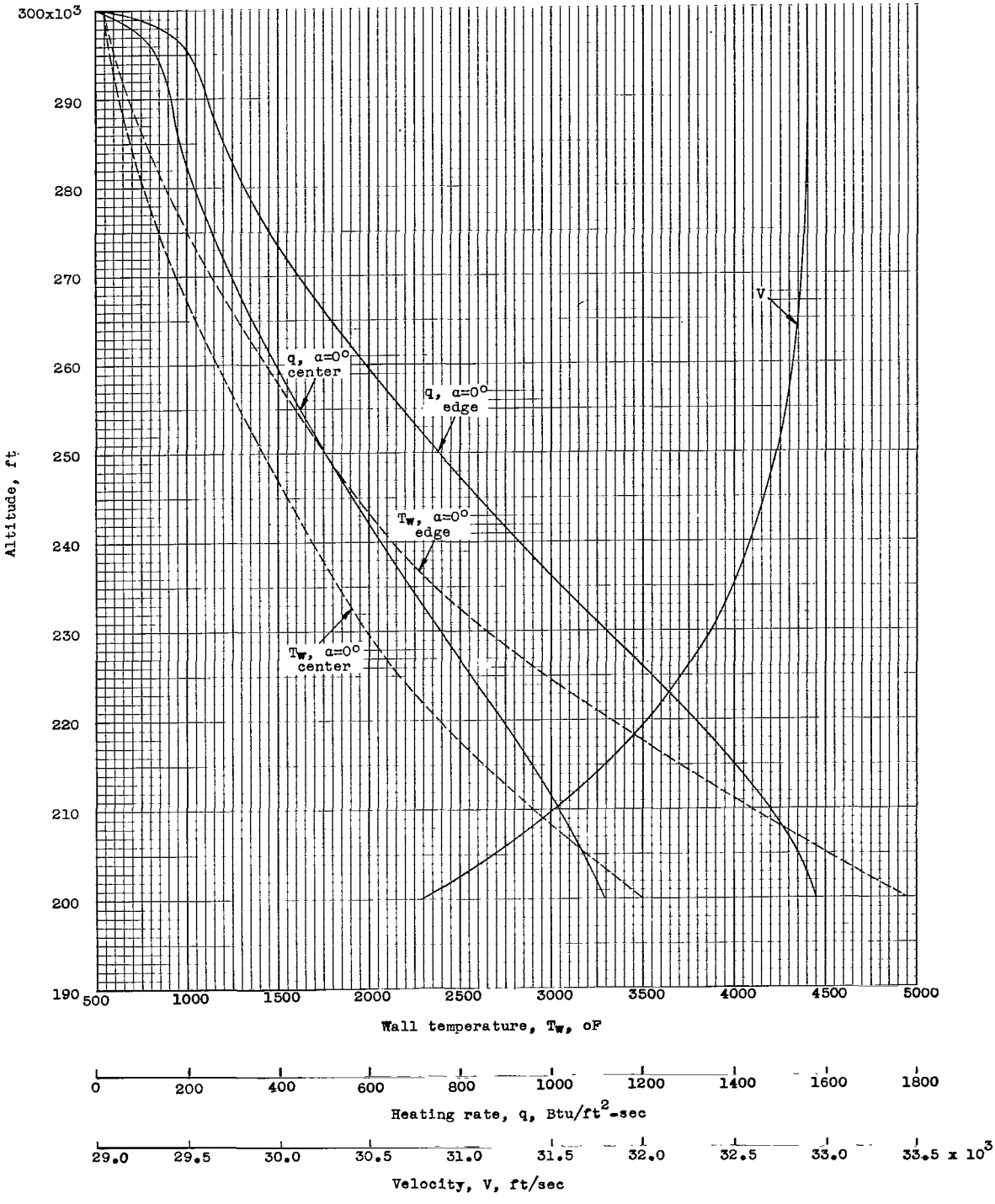


Figure 18.- Variation of calculated heating rates, velocity, and wall temperature with altitude for pellet.

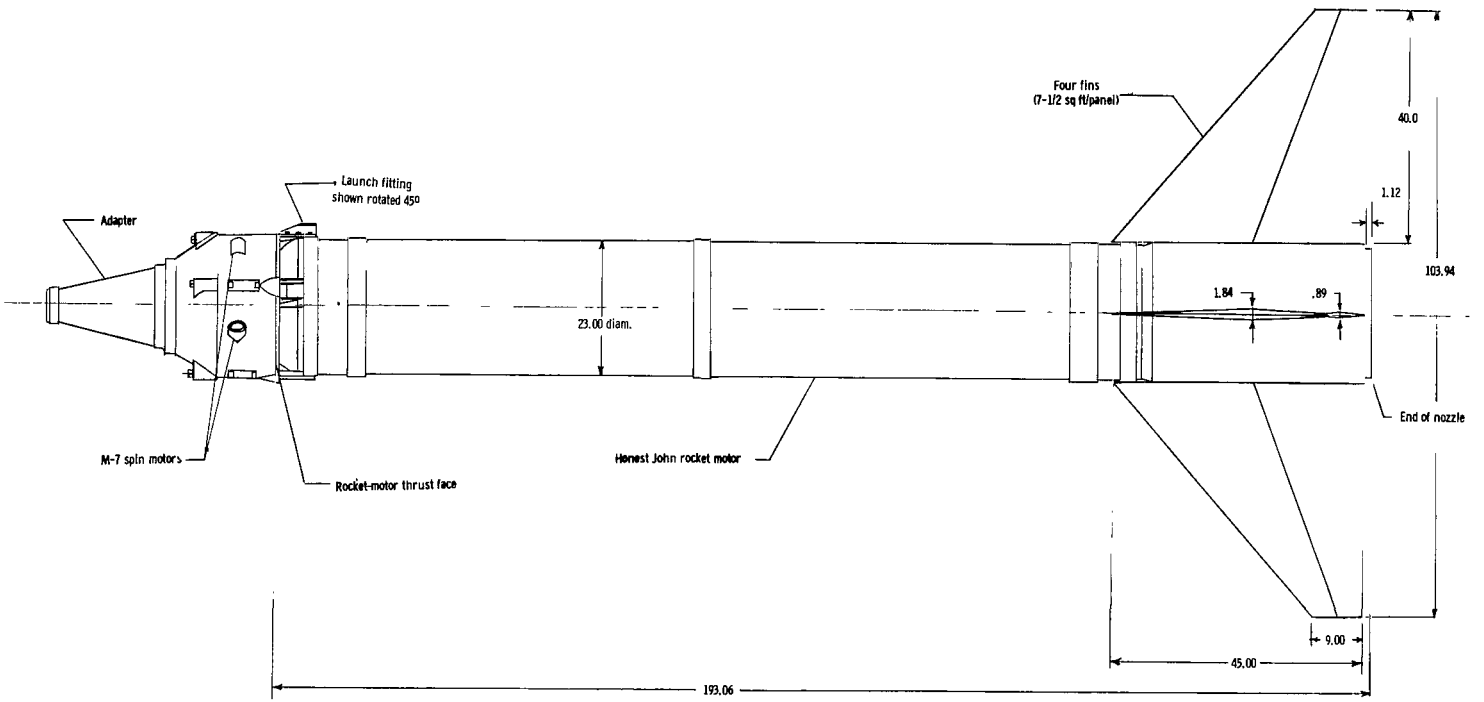


(a) Sketch of first-stage rocket motor.

Figure 19.- Sketch of booster rocket motors. All dimensions are in inches.

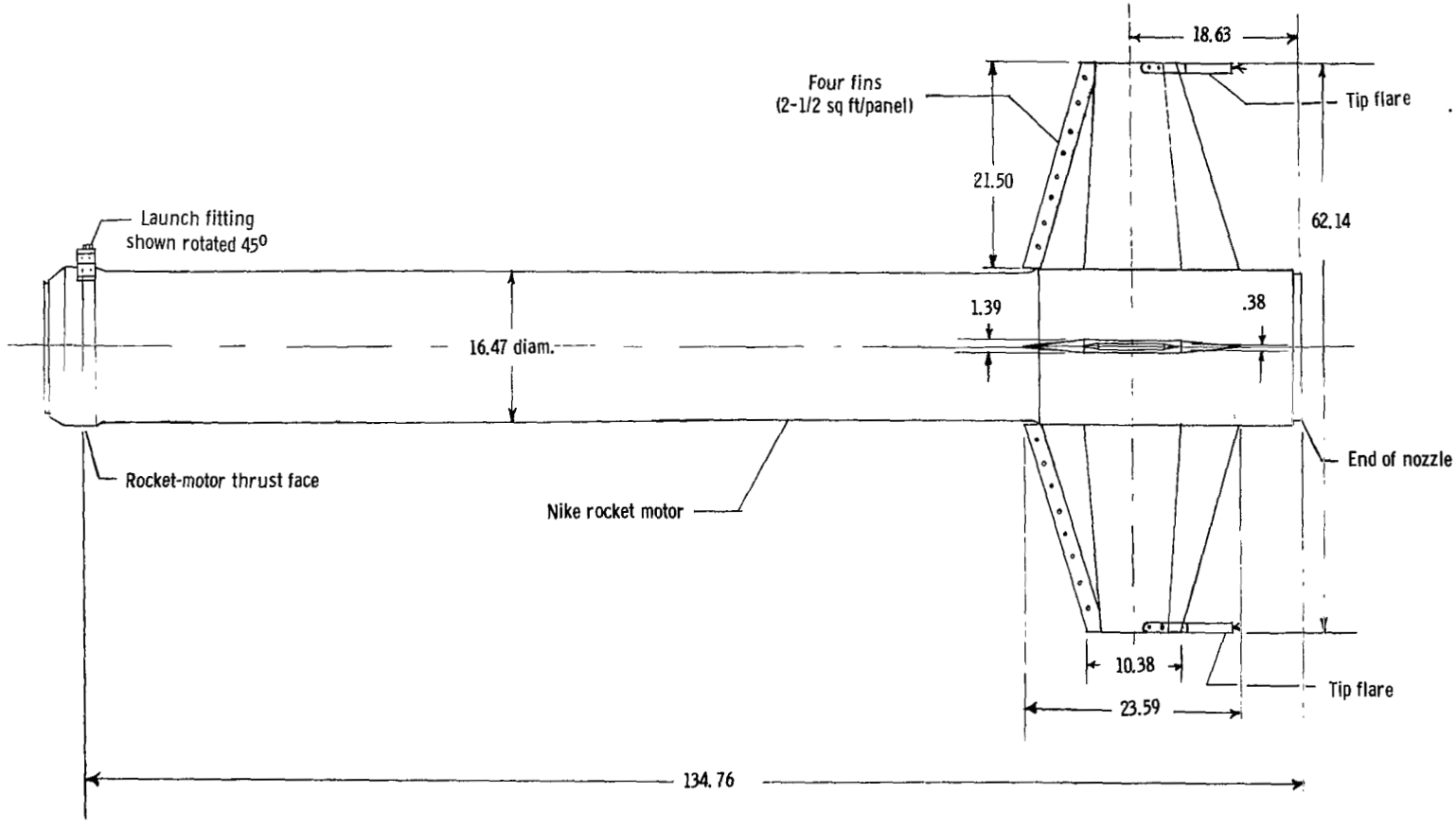


(b) Sketch of second-stage rocket motor.

Figure 19.- Continued.

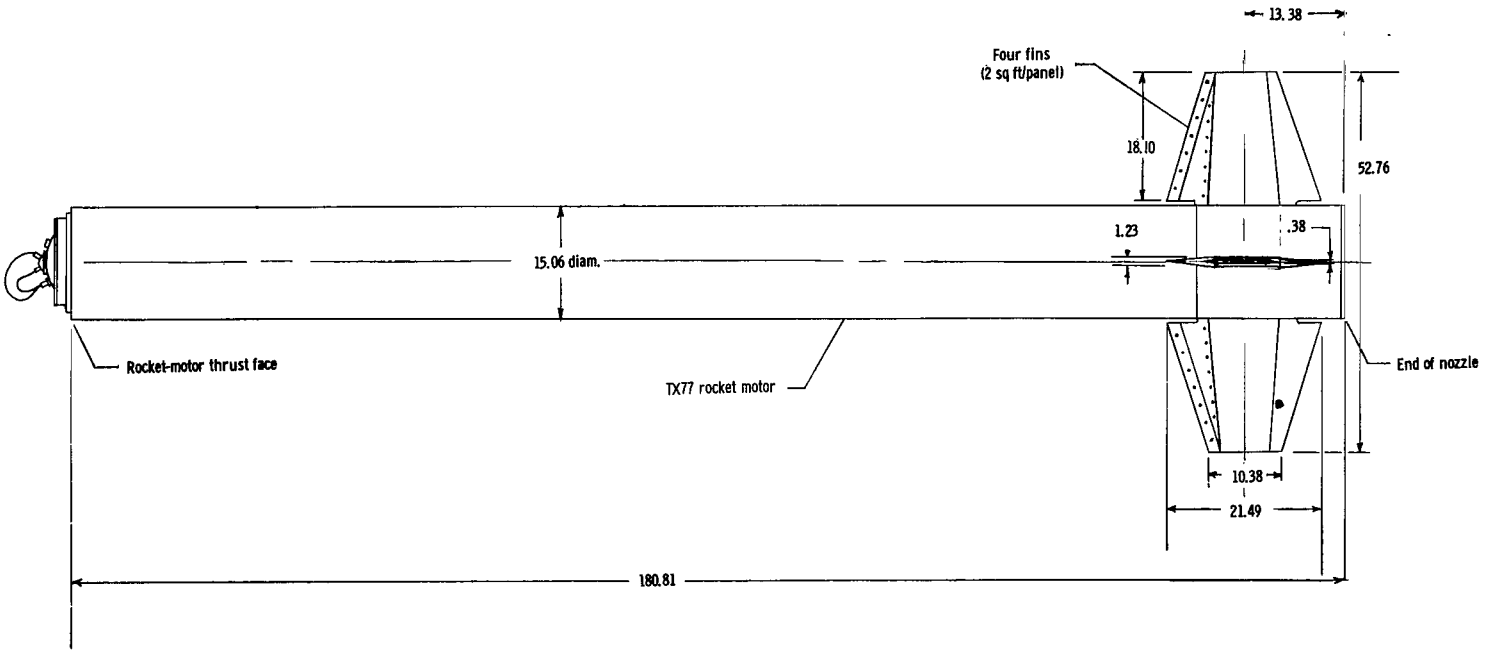


(c) Sketch of third-stage rocket motor.

Figure 19.- Concluded.

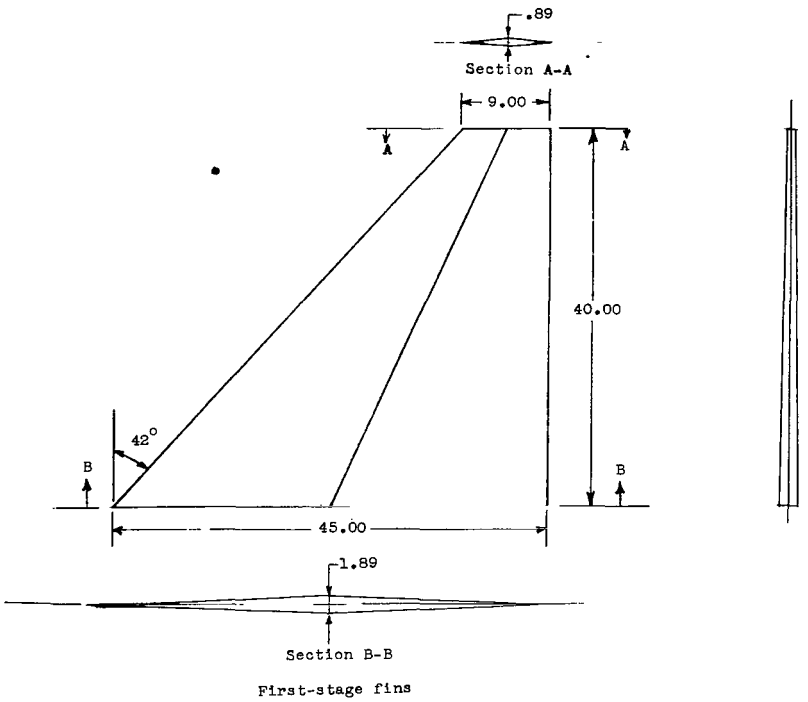


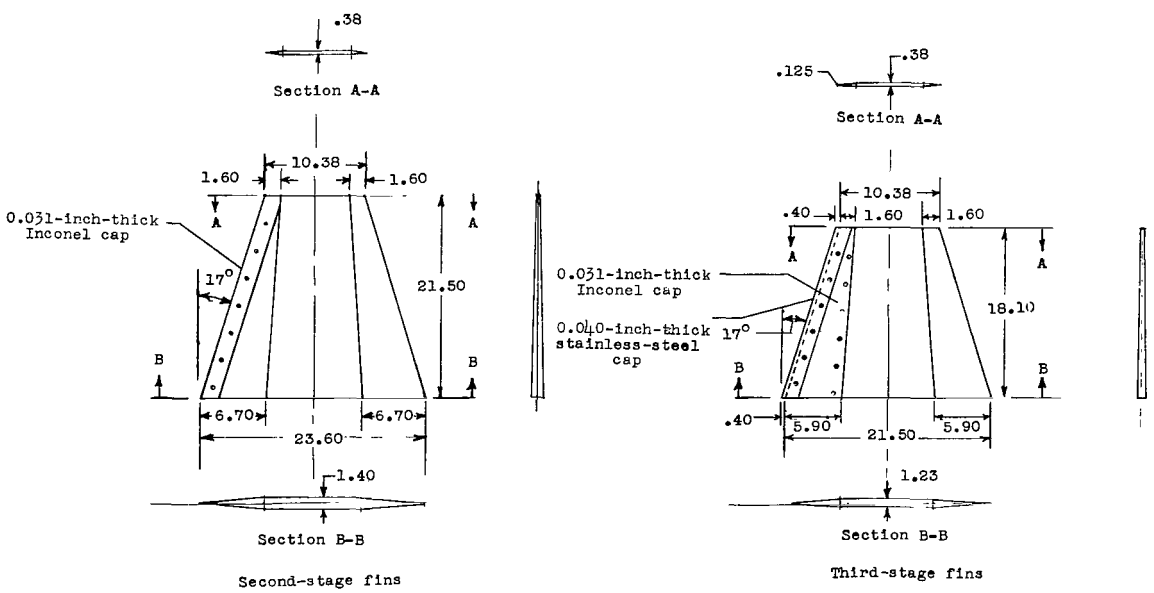


Figure 20.- Sketch of fins for first, second, and third stages. All dimensions are in inches.

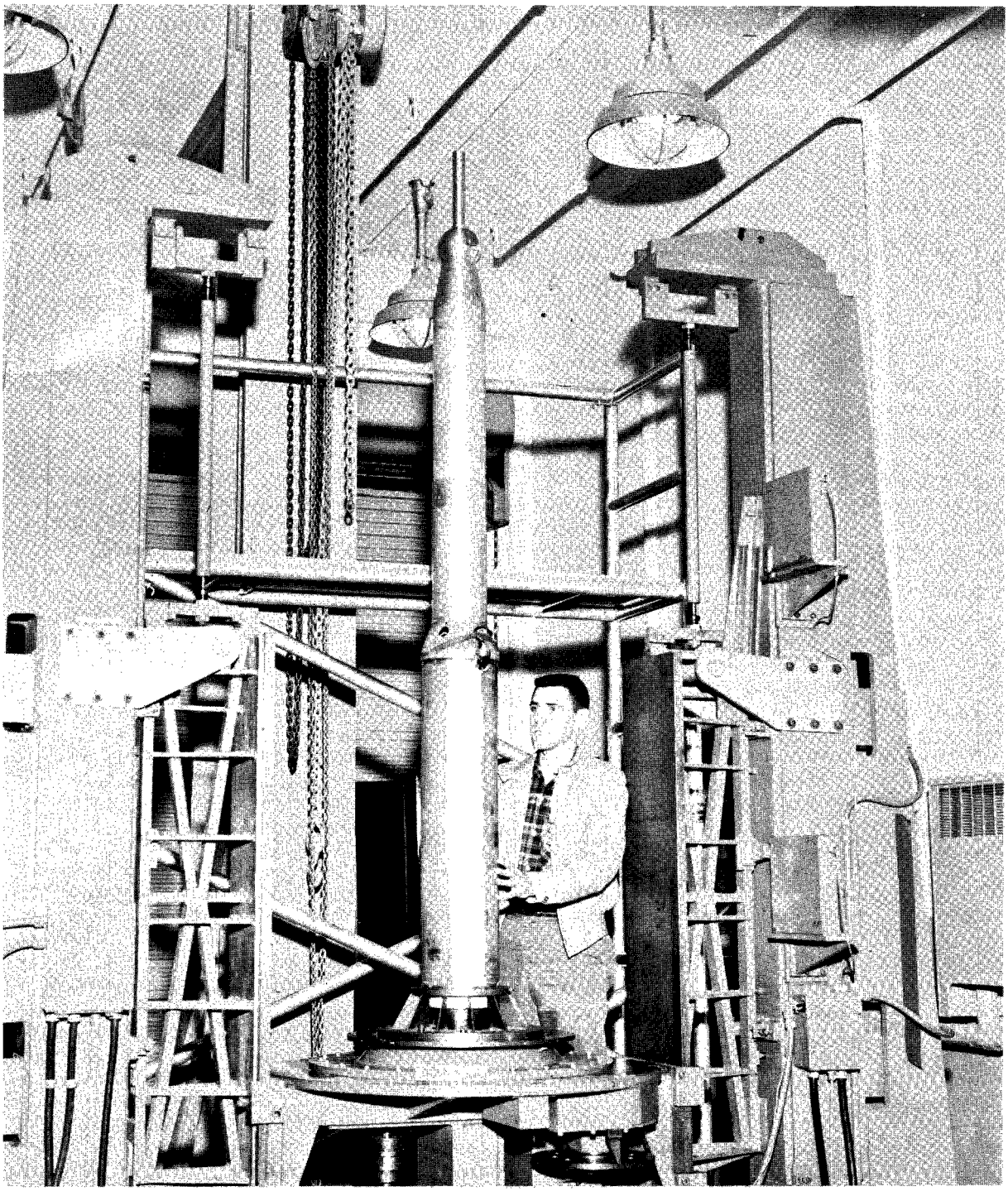

(a) Fourth, fifth, sixth, and seventh stages on dynamic balancing machine.

Figure 21.- Photographs of combination of components on dynamic balancing machine. L-61-3081

(b) Fifth, sixth, and seventh stages on dynamic balancing machine. L-61-3076

Figure 21.- Concluded.



NASA-Langley, 1964 L-3858

2/12/65

*"The National Aeronautics and Space Administration . . . shall . . . provide for the widest practical appropriate dissemination of information concerning its activities and the results thereof . . . objectives being the expansion of human knowledge of phenomena in the atmosphere and space."*

—National Aeronautics and Space Act of 1958

# NASA SCIENTIFIC AND TECHNICAL PUBLICATIONS

TECHNICAL REPORTS: Scientific and technical information considered important, complete, and a lasting contribution to existing knowledge.

TECHNICAL NOTES: Information less broad in scope but nevertheless of importance as a contribution to existing knowledge.

TECHNICAL MEMORANDUMS: Information receiving limited distribution because of preliminary data, security classification, or other reasons.

CONTRACTOR REPORTS: Technical information generated in connection with a NASA contract or grant and released under NASA auspices.

TECHNICAL TRANSLATIONS: Information published in a foreign language considered to merit NASA distribution in English.

TECHNICAL REPRINTS: Information derived from NASA activities and initially published in the form of journal articles or meeting papers.

SPECIAL PUBLICATIONS: Information derived from or of value to NASA activities but not necessarily reporting the results of individual NASA-programmed scientific efforts. Publications include conference proceedings, monographs, data compilations, handbooks, sourcebooks, and special bibliographies.

*Details on the availability of these publications may be obtained from:*

SCIENTIFIC AND TECHNICAL INFORMATION DIVISION

NATIONAL AERONAUTICS AND SPACE ADMINISTRATION

Washington, D.C. 20546